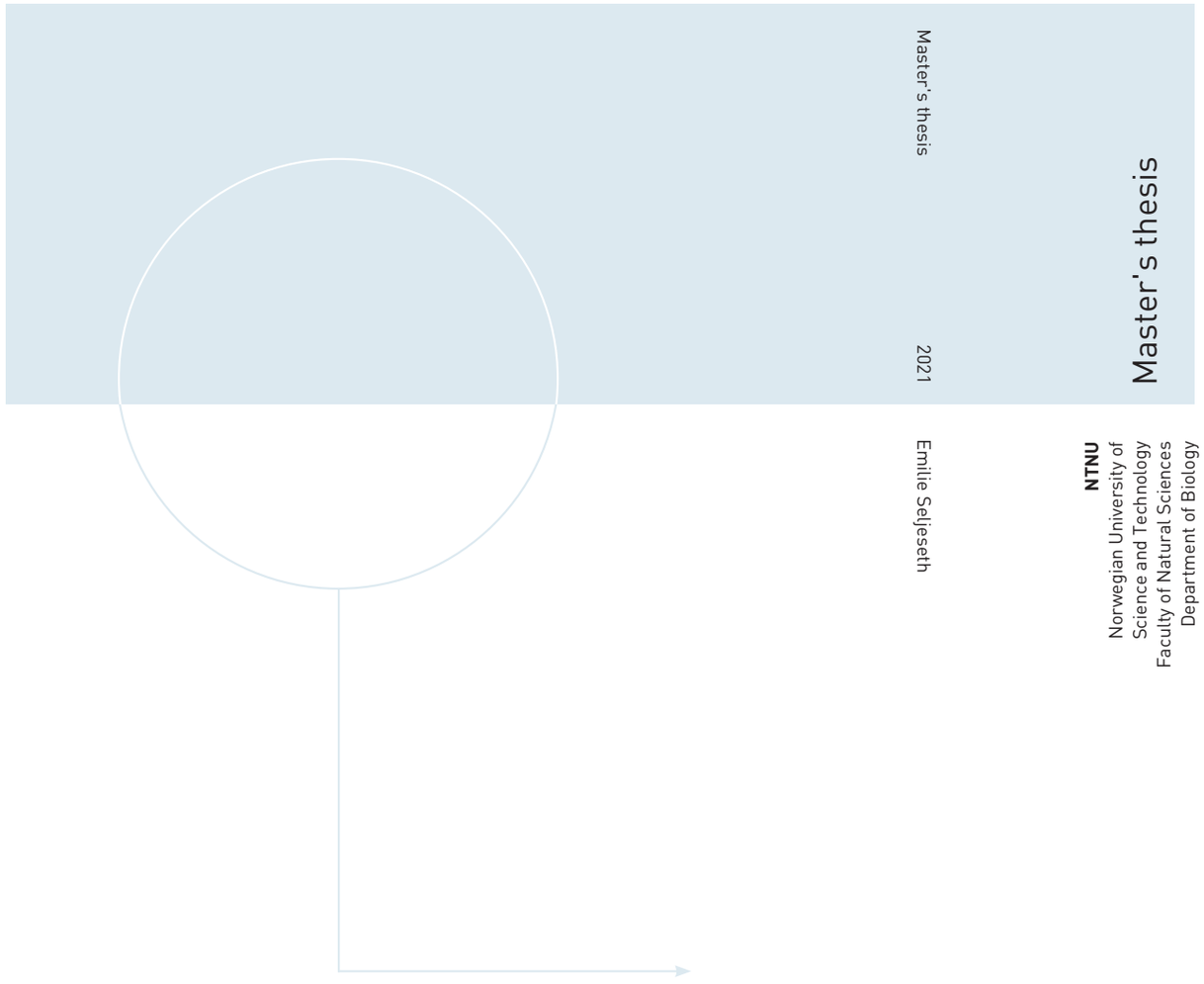

Emilie Seljeseth

Characterization of *in vitro* polarized human neutrophils - a model for testing how cancer cells affect neutrophil polarization

May 2021

NTNU
Norwegian University of
Science and Technology

NTNU
Norwegian University of
Science and Technology

NTNU

Norwegian University of
Science and Technology

Characterization of *in vitro* polarized human neutrophils - a model for testing how cancer cells affect neutrophil polarization

Emilie Seljeseth

Master of Science in Biology
Submission date: May 2021
Supervisor: Dr. Nadra Nilsen
Co-supervisor: Dr. Marit Bugge

Norwegian University of Science and Technology
Department of Biology

Acknowledgements

This master's thesis was conducted at the Centre for Molecular Inflammation Research (CEMIR), part of the Department of Clinical and Molecular Medicine (IKOM), at the Norwegian University of Science and Technology (NTNU). The thesis represents the final part of a Master of Science in Biology.

I would like to express my gratitude towards my supervisors Dr. Nadra Nilsen and Dr. Marit Bugge for their support and guidance throughout this project. To Nadra, thank you for giving me the opportunity to conduct my thesis at CEMIR and to work on this exciting project as part of your research group. I am also thankful to the staff and researchers at CEMIR for being so welcoming and always willing to lend a helping hand.

Trondheim, May 2021
Emilie Seljeseth

Abstract

Neutrophils are the most abundant leukocytes in the human circulation and the first cells to be recruited to sites of infection and inflammation. These innate immune cells are major players in host immunity and have traditionally been considered a homogenous population of cells, whose main purpose is to protect against infections. However, accumulating evidence has revealed a larger heterogeneity for these cells than first presumed and the observation that neutrophils play important roles in the pathogenesis of various diseases has sparked a renewed interest in neutrophil biology. Cancer is a condition in which the number of neutrophils in circulation increases, often correlating with poor prognosis, and several studies report an enrichment of neutrophils in the tumor microenvironment (TME). Further, neutrophils have been observed to become polarized in the TME and can acquire both anti- (N1) and pro-tumor (N2) phenotypes, which may offer possibility for therapeutic targeting.

Because neutrophils have short lifespans in culture and are prone to spontaneous activation and apoptosis, most studies on neutrophils in cancer have been based on murine models. However, because there are biological differences between human and murine neutrophils, the results observed in murine tumor systems may not translate to humans. In this study, a newly reported method for *in vitro* polarization of human neutrophils into cells with N1- and N2-like characteristics was assessed and verified. In addition, the N1- and N2-polarized cells were characterized further and were revealed to exhibit distinct expressional profiles. Finally, the *in vitro* polarization model was further employed to investigate the polarization potential of colon cancer cells. The preliminary findings indicated that TLR3-activation in colon cancer cells shifts polarization towards an N1-like phenotype and demonstrated a use for this model in the elucidation of how inflammatory signaling affect neutrophil polarization.

Sammendrag

Nøytrofile er de mest tallrike leukocyttene i den menneskelige sirkulasjonen og de første cellene som rekrutteres til infeksjons- og betennelsessteder. Disse medfødte immuncellene er hovedaktører i vertsimmuniteten og har tradisjonelt blitt ansett som en homogen populasjon av celler, hvis hovedformål er å beskytte mot infeksjoner. Imidlertid har økende bevis avslørt en større heterogenitet for disse cellene enn først antatt, og observasjonen om at nøytrofile spiller viktige roller i patogenesen av forskjellige sykdommer har utløst en fornyet interesse for nøytrofilbiologi. Kreft er en sykdom der antall nøytrofile i sirkulasjonen øker, noe som ofte korrelerer med dårlig prognose, og flere studier har rapportert en økning av nøytrofile i tumor mikromiljøet. Videre har nøytrofile blitt observert i å bli polariserte i tumor mikromiljøet og kan tilegne seg både anti- (N1) og pro-tumor (N2) fenotyper, noe som kan åpne muligheten for målrettede terapier.

Fordi nøytrofile har kort levetid i kultur og er sensitiv for spontan aktivering og apoptose, har de fleste studier på nøytrofile i kreft vært basert på musemodeller. Likevel, fordi det er biologiske forskjeller mellom nøytrofile i mus og mennesker kan ikke resultatene som observeres i tumor-systemer basert på mus direkte overføres til mennesker. I denne studien ble en nylig rapportert metode for *in vitro* polarisering av humane nøytrofile til celler med N1- og N2-lignende egenskaper vurdert og verifisert. I tillegg ble N1- og N2-polariserte celler karakterisert ytterligere og demonstrert til å utvise distinkt genuttrykk. Til slutt ble *in vitro* polariseringsmodellen benyttet til å undersøke polariseringspotensialet til tykktarmskreftceller. De foreløpige funnene avslørte at TLR3-aktivering i tykktarmskreftceller muligens forskyver polarisering mot en N1-fenotype og demonstrerte at denne modellen kan brukes til å undersøke hvordan inflammatoriske signalveier virker inn på polarisering av nøytrofile.

Table of Contents

List of figures

List of Tables

Abbreviations

ADCC	Antibody-dependent cell-mediated cytotoxicity
AGO	Argonaute
ANOVA	Analysis of variance
APC	Allophycocyanin
ARG1	Arginase 1
BLT1	Leukotriene B_4 receptor 1
BM	Bone marrow
BSA	Bovine Serum Albumin
BV	Brilliant Violet
C5a	Complement component 5a
C5aR1	C5a receptor 1
CD	Cluster of differentiation
CO_2	Carbon dioxide
CRC	Colorectal cancer
CXCL	C-X-C chemokine ligand
CXCR	C-X-C chemokine receptor
DAMP	Damage-associated molecular pattern
DN	Double-negative
DPBS	Dulbecco's Phospate Buffered Saline
dsRNA	Double-stranded RNA
ECM	Extracellular matrix
ELISA	Enzyme-linked immunosorbent assay
FACS	Fluorescence-activated cell sorting
FCS	Fetal calf serum
FITC	Fluorescein isothiocyanate
FSC	Forward scatter
FVD	Fixable Viability Dye
G-CSF	Granulocyte colony-stimulating factor
G-MDSC	Granulocytic myeloid-derived suppressor cell
GMP	Granulocyte-monocyte progenitor
GPCR	G-protein coupled receptor
HLA-DR	Human leukocyte antigen-DR
H. pylori	*Heliobacter pylori*
HBSS	Hank's Balanced Salt Solution
HCl	Hydrochloric acid
HEPES	Hydroxyethyl piperazineethanesulfonic
HI	Heat-inactivated
HRP	Horseradish peroxidase
HSC	Hematopoietic stem cell
IBD	Inflammatory bowel disease
ICAM-1	Intercellular adhesion molecule-1
IFNβ	Interferon beta
IFI35	Interferon induced protein 35
IFNγ	Interferon gamma
IL-10	Interleukin-10
IL-6	Interleukin-6
LPS	Lipopolysaccharide
LTB_4	Leukotriene B_4
MFI	Median fluorescence intensity
MIF	Macrophage migration inhibitory factor

miRNA	Micro RNA
MMP	Matrix-metalloproteinase
MPO	Myeloperoxidase
NADPH	Nicotinamide adenine dinucleotide phosphate
NE	Neutrophil elastase
NET	Neutrophil extracellular trap
NF-κB	Nuclear factor kappa-light chain enhancer of activated B-cells
NLR	Neutrophil to lymphocyte ratio
O_2	Oxygen
OSM	Oncostatin M
PAMP	Pathogen-associated molecular pattern
PBMC	Peripheral mononuclear cell
PE	Physcoerythrin
Pen-Strep	Penicillin-Streptomycin
PGE_2	Prostaglandin E_2
PMT	Photomultiplier tube
poly(I:C)	Polyinosinic:polycytidylic acid
PRR	Pattern recognition receptor
Q-VD-OPh	Quinoline-Val-Asp-Difluorophenoxymethyl ketone
RBC	Red blood cell
RISC	RNA-induced silencing complex
RNAi	RNA interference
ROS	Reactive oxygen species
RPMI 1640	Roswell Park Memorial Institute 1640
RT-PCR	Reverse transcription-quantitative polymerase chain reaction
S100	S100 calcium-binding protein
Siglec-1	Sialic acid binding Ig-like lectin 1
siRNA	Small interfering RNA
SSC	Side scatter
TAM	Tumor-associated macrophage
TAN	Tumor-associated neutrophil
TGFβ	Transforming growth factor beta
TAP-2	Transporter 2
TLR	Toll-like receptor
TMB	Tetramethylbenzidine
TME	Tumor microenvironment
TNFα	Tumor necrosis factor alfa
VEGF	Vascular endothelial growth factor

1. Introduction

Neutrophils (also known as polymorphonuclear cells) are the most abundant leukocytes in the human circulation and the body's first line of defense against invading pathogens (Mayadas et al., 2014). They belong to the innate arm of immunity and are relatively short-lived cells that most often die while performing their life-saving functions. These granulocytes are major players in host immunity, where they extravasate from the circulation into tissues to capture and kill intruding microbes. In addition, they are potent mediators of inflammation and actively shape the responses of other immune cells. Traditionally, the focus on neutrophils has been on their roles in protective immunity. However, accumulating evidence demonstrate that neutrophils play important roles in the pathogenesis of various diseases as well, most notably in cancer (Coffelt et al., 2016).

1.1. Neutrophils in immunity

The immune system consists of a complex network of organs, tissues and cells, and the substances that they produce. Every day, countless immune cells patrol the body for signs of infection and abnormalities. Neutrophils are the first cells to be recruited from circulation to sites of infection and inflammation and constitute as much as 50-70% of all circulating leukocytes (Mayadas et al., 2014). These innate immune cells develop from hematopoietic stem cells (HSC)s in the bone marrow (BM) at numbers close to 10^{11} cells per day (Dancey et al., 1976) and form a large storage pool of cells that can be quickly mobilized during infectious or inflammatory episodes (Semerad et al., 2002).

The exact mechanisms of neutrophil development from HSCs are not fully understood but the current model suggests that HSCs, through a series of differentiation steps, transform into granulocyte-monocyte progenitor (GMP) populations which in turn give rise to neutrophils. These GMPs have both granulocyte and monocyte potential but commit to the neutrophil lineage under the influence of granulocyte colony-stimulating factor (G-CSF) (von Vietinghoff and Ley, 2008) by turning into myeloblasts. The developing neutrophil then follows a maturation program that includes the stages of promyelocyte, myelocyte, metamyelocyte and band cell before mature neutrophils appear (Cowland and Borregaard, 2016)

Neutrophils take their cues directly from the infectious organism, from tissue macrophages, or inflammatory mediators. Under homeostatic conditions, they enter the circulation, migrate to tissues where they complete their functions and finally are cleared by tissue phagocytes (Rosales, 2018). They are essential in host defense, particularly against bacteria and fungi (Ermert et al., 2009), and are activated in response to pathogen- (PAMP)s and damage-associated (DAMP)s molecular patterns, immune complexes, complement and cytokines (Mayadas et al., 2014). Once activated, they display a battery of effector mechanisms that include the production of reactive oxygen species (ROS), release of

cytotoxic granule contents, formation of neutrophil extracellular traps (NET)s and phagocytosis of microbes (Mayadas et al., 2014). In addition, neutrophils are potent inducers of inflammation and attract and shape the activities of other immune cells by releasing inflammatory mediators **(Figure 1.1)**.

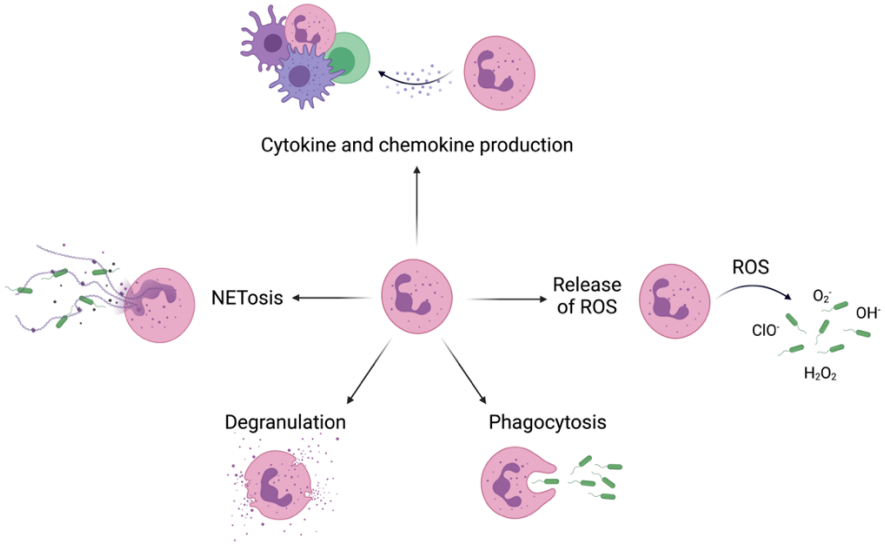

Figure 1.1. Overview of neutrophil effector functions. Neutrophils can perform several effector functions in response to activating stimuli. Production of reactive oxygen species (ROS) is mediated through the nicotinamide adenine dinucleotide phosphate (NADPH) oxidase complex. Phagocytosis involves the ingestion and intracellular degradation of microorganisms. Degranulation is the release of hydrolytic enzymes and antimicrobial peptides from premade granules. NETosis is a form of cell death in which neutrophils expulse their DNA together with histones and granular or cytoplasmic proteins to form neutrophil extracellular traps (NET)s, which they use to trap and kill microorganisms. Finally, neutrophils release cytokines and chemokines that modulate and attract other immune cells to sites of infection and inflammation. *Created with BioRender.com*

The essential role of neutrophils in protective immunity is clearly illustrated in individuals with neutropenia (e.g., as result of chemotherapy or birth defects), which are highly susceptible to severe infections (Dale, 2009). However, neutrophils can play a dual role. When deployed at the wrong time and place, their antimicrobial and immunomodulatory functions can act as a driving force for the initiation and progression of disease-associated inflammation (Mayadas et al., 2014). Although traditionally considered as rigid, pre-programmed effector cells whose main function is to protect against infections, accumulating studies have reported a larger heterogeneity for these cells than first presumed and different phenotypes with distinct surface markers, maturation states, locations and functions have been described under both healthy and pathological conditions (Liew and Kubes, 2019).

1.2. Neutrophils in Cancer

Cancer is not the solo performance of malignant cells (Joyce, 2005). In addition to the cancerous cells themselves, the tumor microenvironment (TME) contains normal cells from the host such as endothelial cells, stromal fibroblasts, cells composing blood and lymphatic vessels and infiltrating immune cells (Anderson and Simon, 2020). Traditionally, the cells of our immune system are viewed as protectors that eliminate invading pathogens and malignancies. However, there is a general agreement that a dysregulated inflammatory response contribute to the formation, progression and spread of cancer (Rossi et al., 2021) and that factors present in the TME can polarize, or activate, immune cells into subsets that aid in malignant tumor progression (Johansson et al., 2008).

Neutrophils constitute a significant portion of the immune cell types infiltrating the TME (Shen et al., 2014, Wu et al., 2019) and a high neutrophil to lymphocyte ratio (NLR) is often observed in the circulation of cancer patients with more advanced disease (Guthrie et al., 2013, Schmidt et al., 2005, Sr et al., 2005, Tavakkoli et al., 2019). These cells play significant roles in linking inflammation and cancer and have been demonstrated to support tumor progression by mechanisms that involve promoting immunosuppression, angiogenesis and metastasis (Coffelt et al., 2016). Still, other studies have shown that neutrophils also possess anti-tumor properties including direct cytotoxicity towards cancer cells (Granot et al., 2011). Given this dual role, an elucidation of the mechanisms that drive the generation of pro- and antitumor neutrophils in different cancers could open the door to new treatment opportunities.

1.2.1. Recruitment to the tumor-microenvironment

The neutrophil migration cascade relies on chemoattractants and their receptors. In humans, neutrophil chemoattractants are divided into four biochemical subfamilies, which are chemokines (e.g., C-X-C chemokine ligand 1 [CXCL1]), chemotactic lipids (e.g., leukotriene B_4 [LTB_4]), complement anaphylatoxins (e.g., complement component 5a [C5a]) and formyl peptides (e.g., N-formyl-Met-Leu-Phe). They all function by activating G-protein coupled receptors (GPCR)s (Metzemaekers et al., 2020). Circulating neutrophils are recruited into tissues when they sense chemoattractants or other activating stimuli on endothelial cells (Kolaczkowska and Kubes, 2013). In most tissues, the recruitment cascade involves the sequential steps of tethering to the endothelial wall, rolling, firm adhesion, crawling and finally transmigration between or through endothelial cells. Tethering and rolling are mostly selectin-dependent, whereas adhesion, crawling and transmigration depend on integrin interactions (Kolaczkowska and Kubes, 2013). Emigrated neutrophils then continue their journey by following the chemotactic gradient.

Cells in the TME attract neutrophils to the tumor by producing neutrophil-attracting factors. Tumor cells produce many chemokines that are chemoattractants for neutrophils, including CXCL1-2 and CXCL5-8 that recruit neutrophils to the tumor through interactions with C-X-C chemokine receptors 1 and 2 (CXCR1-2) (Lazennec and Richmond, 2010). Also, the expression of CXCL10 by many of the cells present in the TME, recruit neutrophils through their CXCR3 receptors (Wightman et al., 2015). Many tumors also display upregulation of complement proteins and excessive complement activation, which can directly recruit neutrophils to the TME through C5a receptor 1 (C5aR1) (Zhang et al., 2019). In addition, complement activation also recruits neutrophils indirectly by stimulating epithelial and endothelial cells to release the chemotactic lipid LTB_4, which recruit neutrophils through the leukotriene B4 receptor 1 (BLT1) (Allendorf et al., 2005). Production of CXCL1-2, tumor necrosis factor alfa (TNFα) and interferon gamma (IFNγ) by activated T-cells also, either directly or indirectly, recruit more neutrophils to the tumor (Uribe-Querol and Rosales, 2015). Finally, activated neutrophils produce many of the chemoattractants that they themselves respond to and can create a positive loop for recruitment (Nemeth and Mocsai, 2016).

1.2.2. Pro- and antitumor neutrophils

The major theme that has emerged from studying neutrophils in cancer is that not all neutrophils are equal and that these cells display opposing functions depending on factors produced by the TME (Coffelt et al., 2016). Studies based on murine models have shown that the pleiotropic cytokine transforming growth factor beta (TGFβ) promote the generation of pro-tumor neutrophils with T-cell suppressive abilities (Casbon et al., 2015, Fridlender et al., 2009), whereas interferon beta (IFNβ) supports anti-tumor properties (Jablonska et al., 2010). In addition, the physiological conditions of the TME, such as hypoxic and acidic conditions, may also play a role in polarization as cytotoxic anti-tumor neutrophils have been shown to acquire a pro-tumor phenotype along with tumor progression (Mishalian et al., 2013).

Particularly two subpopulations of neutrophils have been the center of attention in cancer research, namely granulocytic myeloid-derived suppressor cells (G-MDSC)s, that accumulate in the circulation and in the vicinity of the TME, and tumor-associated neutrophils (TAN)s, which infiltrate solid tumors (Nagaraj and Gabrilovich, 2010, Fridlender and Albelda, 2012). The relationship between these subpopulations is still a matter of debate but a high frequency of either seems to be related to poor prognosis in several cancers (Ai et al., 2018, Manfroi et al., 2018). Both of these populations have been shown to display tumor-supporting immunosuppressive behaviors but whereas G-MDSCs are described in the pro-tumor context, TANs have been reported to also display antitumor properties (Granot et al., 2011, Matlung et al., 2018). Some studies have proposed that TANs are simply tissue-based G-MDSCs.

However, these cells are significantly different in their transcriptional activities, supporting that they belong to two separate populations of cancer-related neutrophils (Fridlender et al., 2012).

1.2.3. Tumor-associated neutrophils: phenotypes and functions

Following stimulation in the TME, TANs gain the ability to perform activities that suppress or promote tumor progression and display distinct surface markers, secretion profiles and effector functions (Coffelt et al., 2016). In analogy to tumor-associated macrophages (TAM)s, which are known to polarize into an M1 phenotype with antitumor activities or an M2 phenotype with protumor functions (Mills et al., 2000), TANs are classified as antitumor N1 or protumor N2 (Fridlender et al., 2009). Still, it is important to acknowledge that the M1/M2 and N1/N2 classification represent an *in vitro* extremization of the *in vivo* setting and that TAMs and TANs rather likely exist in a continuum of activation states that are not necessarily fixed (Atri et al., 2018). In fact, *in vitro* generated M1- and M2-like cells have been shown to undergo reversible changes when exposed to appropriate stimuli (Xu et al., 2013, Tarique et al., 2015), but the question of whether TANs adapt reversible activation states is still not clear.

In murine tumors, the N1 and N2 phenotypes can be distinguished morphologically as N1 TANs display hyper-segmented nuclei, whereas the nuclei of N2 TANs are more circular (Fridlender et al., 2009) **(Figure 1.2)**. Antitumor N1 TANs are further characterized by an increased cytotoxicity towards tumor cells by increased production of ROS and immunostimulatory TNFα (Fridlender et al., 2009). These cells also upregulate their expression of the cell adhesion molecule cluster of differentiation 54 (CD54/ICAM-1), which could enable these cells to prime and activate T-cells (Eruslanov et al., 2014). In addition, antitumor TANs can recognize antibodies that bind to tumor antigens through their FC-receptors and destroy the tumor cell through antibody-dependent cell-mediated cytotoxicity (ADCC) (Uribe-Querol and Rosales, 2015).

Protumor N2 TANs are characterized by increased production of Arginase 1 (ARG1), which can suppress T-cells by depleting extracellular arginine, an essential amino acid for proper T-cell activation (Fridlender et al., 2009). Other protumor functions described include the production of a large number of molecules that aid in malignant tumor progression. The granular enzyme matrix-metalloproteinase-9 (MMP-9) support angiogenesis by releasing vascular endothelial growth factor (VEGF) from the extracellular matrix (ECM) (Ebrahem et al., 2010). In addition, the proinflammatory interleukin-6 (IL-6)-like cytokine oncostatin M (OSM) has been demonstrated to induce VEGF production in breast cancer cells (Queen et al., 2005). Further, neutrophil elastase (NE), another granule-residing proteinase, has been shown to promote cancer proliferation when murine neutrophils were co-cultured with lung cancer cells (Houghton et al., 2010). Finally, neutrophils may aid in metastasis through dissemination

of escaping tumor cells by the action of MMPs (Deryugina and Quigley, 2006) and can trap and seed circulating tumor cells through NETosis (Najmeh et al., 2017).

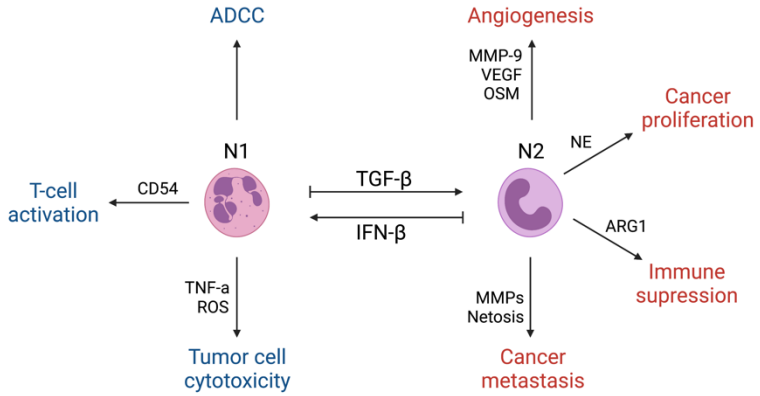

Figure 1.2. Anti- and protumor functions of tumor-associated neutrophils. Tumor-associated neutrophils (TAN)s can be polarized in their activities and perform functions that suppress or aid in malignant tumor progression. Antitumor, or N1 TANs, can suppress tumorigenesis through the production of mediators that are cytotoxic to tumor cells such as tumor necrosis factor alfa (TNFα) and reactive oxygen species (ROS). These cells also recognize antibodies that bind to tumor antigens and can mediate antibody-dependent cell-mediated cytotoxicity (ADCC). In addition, N1 TANs upregulate their expression of CD54/ICAM-1 and may contribute to the priming of T-cells. Pro-tumor, or N2 TANs, suppress T-cells by producing high amounts of Arginase 1 (ARG1). They also contribute to angiogenesis by matrix-metalloproteinase-9 (MMP-9)-mediated release of vascular endothelial growth factor (VEGF) from the extracellular matrix (ECM). In addition, neutrophils can produce the cytokine oncostatin M (OSM), which can induce VEGF production in cancer cells. Neutrophils can also support proliferation of cancer cells through production of neutrophil elastase (NE). Finally, N2 TANs contribute to metastasis through dissemination of tumor cells by MPPs and seeding of circulating tumor cells by the production of neutrophil extracellular traps (NETosis). *Figure based on Wang et al., 2018. Created with BioRender.com*

1.2.4. Tumor-associated neutrophils and inflammatory signaling in colorectal cancer

Neutrophils infiltrate the TME of many solid tumors and TANs are associated with unfavorable conditions in cancers such as colorectal, lung, kidney, liver, head and neck (Rao et al., 2012, Shen et al., 2014, Galdiero et al., 2016). Colorectal cancer (CRC) affects the colon and rectum and is the 4th most frequent and 2nd deadliest cancer in Norway (Kreftregisteret, 2021). When investigating the clinical impact of NLR in blood samples from 354 patients with stage I-III colon cancer, Li et al. found that a high pre-surgical NLR was associated with poor prognosis, whereas a high post-surgical NLR was related to a slightly better outcome (Li et al., 2018). The effect of TANs on the prognosis for CRC patients is still unclear. However, high levels of intratumoral neutrophils have been associated with both adverse and improved prognosis (Rao et al., 2012, Berry et al., 2017).

Cells present in the TME can act in an anti-tumorigenic manner and eliminate malignant cells through immunosurveillance but are also able to foster several of the hallmark functions of cancer including angiogenesis, metastasis and proliferative signaling (Hanahan and Weinberg, 2011) by promoting a proinflammatory environment. Inflammation is initiated in response to harmful stimuli when immune receptors recognize various conditions such as infection, tissue damage, toxic substances or irradiation (Medzhitov, 2010). The best studied innate immune receptors are the Toll-like receptors (TLR)s, a class of pattern recognition receptors (PRR)s that recognize PAMPs and DAMPs (Dajon et al., 2017).

CRC is one of the better examples of inflammation-linked tumorigenesis, as illustrated by the high rates of CRC in patients with inflammatory bowel disease (IBD) and *Heliobacter pylori* (*H. pylori*) infection (Liu et al., 2019, Stidham and Higgins, 2018), and TLRs have been described as potent mediators of inflammation in the gut (Ridnour et al., 2013). These receptors are expressed on many cells in the TME, including immune cells and tumor cells, and play opposing roles in different cancers where their activation have been linked to both anti- and pro-tumor responses (Dajon et al., 2017). TLR-signaling can initiate anti-tumor effects by direct induction of tumor cell death and activation of anti-tumorigenic responses by immune cells, but can also lead to the production of several pro-inflammatory cytokines and chemokines, growth factors and anti-apoptotic proteins that support tumor progression by fueling the proinflammatory environment (Dajon et al., 2017).

Activation of surface TLR3 in metastatic colon cancer cells by the synthetic double-stranded RNA (dsRNA) analog polyinosinic:polycytidylic acid (poly(I:C)) has been linked to the production of several pro-inflammatory mediators, including chemokines CXCL1-2, CXCL5-6, CXCL10 and CXCL8, which are chemoattractants for neutrophils (Bugge et al., 2017) (Unpublished data, Bugge et al., 2020). In addition, TLR3-activation in these cells has been shown to recruit neutrophils *in vitro* (Unpublished data, Bugge et al., 2020), suggesting that TLR3 activation in colon cancer cells may play a role in the enrichment of neutrophils in tumors derived from CRC patients. Whether TLR3-activation also contribute to the polarization of neutrophils in CRC is still unclear.

2. Aims

Traditionally, the focus on neutrophils has been on their roles in fighting infections. However, accumulating evidence have revealed that these innate immune cells also play major roles in cancer progression. Neutrophils are enriched in several tumors and have been observed to acquire both anti- (N1) and pro-tumorigenic (N2) phenotypes in response to mediators present in the TME, which may offer opportunities for therapeutic targeting.

Due to the short lifespan of neutrophils in culture and proneness to activation and spontaneous apoptosis, these populations have mainly been studied in murine models. Because there are biological differences between murine and human neutrophils it is important to take into consideration that the neutrophil responses in mouse tumor models may not translate to humans. It is therefore essential to elucidate the molecular mechanisms that drive the generation of N1 and N2 neutrophils in different human cancers and to determine how inflammatory signaling by cells in the TME, including the tumor cells themselves, affect neutrophil polarization. Finally, a characterization of these opposite polarization states on the basis of surface markers, expressional profiles and effector functions is vital for the identification of these subsets in tumor tissue, which may serve as a prognostic factor.

<u>This project aimed to:</u>

1. Evaluate a newly developed method for *in vitro* polarization of human neutrophils into N1-like and N2-like phenotypes

2. Characterize human N1- and N2-like neutrophils based on differential gene expression

3. Investigate whether the *in vitro* polarization model can be used to assess the neutrophil-polarization potential of stimulated colon cancer cells

3. Materials and Methods

3.1. Isolation of primary human neutrophils

Primary human neutrophils were isolated from whole blood using Dextran sedimentation and Lymphoprep density gradient. As first responders of the immune system, neutrophils are easily activated, and successful isolation requires considerable skill and experience. The isolation procedure was therefore performed by Dr. Miriam Giambelucca.

3.1.1. Ethics statement

The collection of human whole blood for experiments was approved by the Regional Committee for Medical and Health Research Ethics in Central Norway (REC Central), The Norwegian Ministry of Education and Research, no. 2009/2245.

3.1.2. Procedure

The procedure was conducted at room temperature and under sterile conditions as summarized in **Figure 3.1**. Venous blood was collected by venipuncture from healthy volunteers into BD Vacutainer Citrate blood collection tubes (BD) **(1)** and centrifuged for 10 minutes at 400 x *g* to separate blood cells from plasma **(2)**. Plasma was discarded **(3)**, and red blood cells (RBC)s were sedimented by incubation with 10 mL Dextran from Leuconostoc ssp. for 30 minutes (2% [Sigma-Aldrich, #31392-50G] diluted in Hank's Balanced Salt Solution [HBSS] [1x, Sigma-Aldrich]) **(4)**. The leukocyte-rich supernatant was collected **(5)** and spun on a bed of 10 mL Lymphoprep (Axis-Shield) for 30 minutes at 600 x *g* to pellet neutrophils and RBCs **(7)** before the supernatant was discarded **(8)** and RBCs were removed by hypotonic lysis **(9)**.

For the lysis, the pellet of RBCs and neutrophils was resuspended in 5 mL sterile water and subsequently transferred into a clean tube containing 31 mL sterile water. Lysis was terminated by the addition of 4 mL HBSS (10x, Sigma-Aldrich). The procedure was performed in less than 30 seconds to limit exposure to hypotonic conditions. Finally, isolated neutrophils were spun for 10 minutes at 600 x *g* and resuspended in complete medium **(10)** (Roswell Park Memorial Institute 1640 medium [RPMI 1640] [SAFC, #R8758] supplemented with 10% fetal calf serum [FCS] [Gibco, #10270-106], 2 mM L-glutamine [Sigma-Aldrich, #56-85-9], 10 mM hydroxyethyl piperazineethanesulfonic acid [HEPES] [Thermo Fisher, #15630056] and X mM Penicillin-Streptomycin [Pen-Strep] [Gibco, #15140122]).

Cell viability was measured to >98% by Tryphan Blue exclusion on a Z2 Coulter Particle Count and Size Analyzer (Beckman Coulter). Neutrophil purity was determined by flow cytometry against T-cell

$CD3^{APC}$, monocyte $CD14^{FITC}$ and granulocyte $CD15^{BV605}$ and $CD66b^{BV421}$ as described in **Section 3.5** and showed <1% contamination with monocytes or T-cells (**Figure 4.1.2 and Figure 4.3.1**).

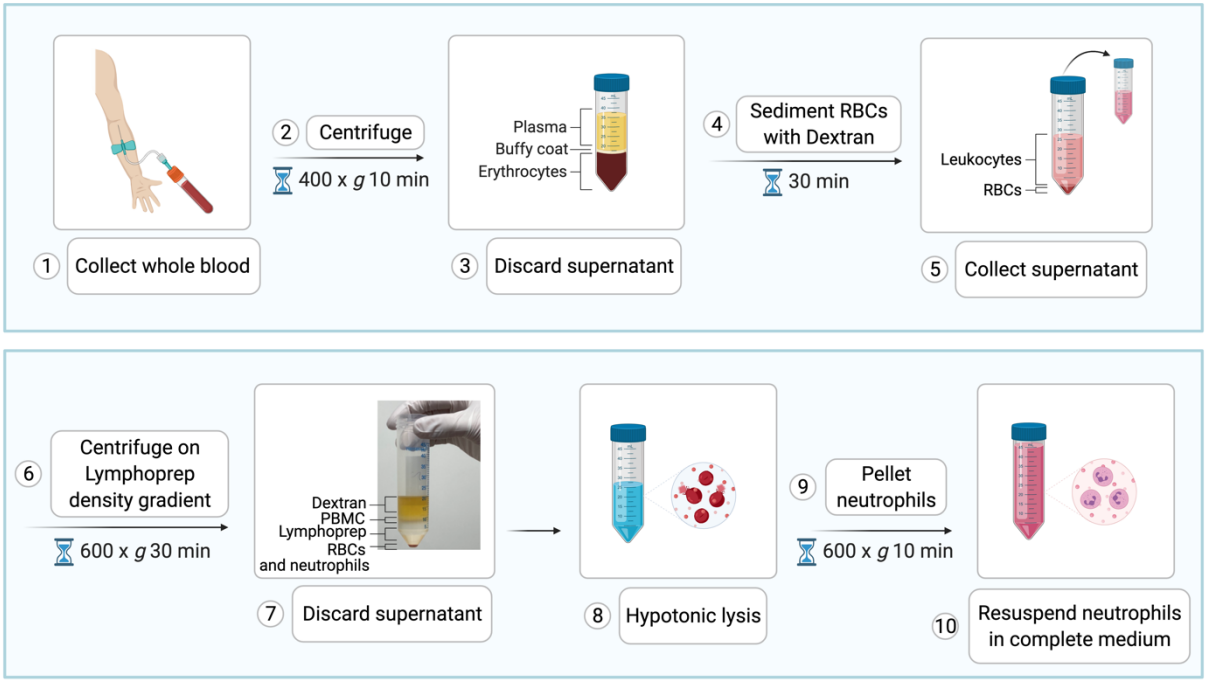

Figure 3.1. Workflow for isolation of primary human neutrophils from whole blood. *Created with BioRender.com*

3.2. Culture and *in vitro* polarization of neutrophils

Isolated neutrophils were polarized into antitumorigenic N1-like and pro-tumorigenic N2-like cells based on a protocol developed by Mareike Ohms et al. (Ohms et al., 2020).

3.2.1. Procedure

Freshly isolated neutrophils were seeded in Corning 24-well plates (4 million cells/mL at 1.875 mL/well) (Corning Life Sciences, #3524) and incubated for 24- or 48h. Polarization towards an N1-like phenotype was conducted in complete medium supplemented with an N1-polarization cocktail containing 100 ng/mL Lipopolysaccharide (LPS) from *Escherichia coli* 0111:B4 (InvivoGen #tlrl-3pelps), 50 ng/mL interferon gamma (IFNγ) (R&D Systems, #285-IF), and 10.000 U/mL interferon beta (IFNβ) (R&D Systems, #8499-IF) at 37°C in a humidified air atmosphere containing 5% carbon dioxide (CO_2). Polarization towards an N2-like phenotype was performed in complete medium supplemented with an N2-polarization cocktail containing 25 mM sodium L-lactate (Merck, #L7022), 10 μM adenosine (Sigma-Aldrich, #A4036), 20 ng/mL transforming growth factor beta (TGFβ) (PeproTech, #100-21), 10 ng/mL interleukin-10 (IL-10) (BioLegend, #571004), 20 ng/mL prostaglandin E_2 (PGE_2) (Tocris, #2296) and 100 ng/mL granulocyte colony-stimulating factor (G-CSF) (PeproTech, #300-23) at 37°C in a humidified hypoxic chamber with 2% oxygen (O_2) and 5% CO_2. The pH of the medium

containing the N2 polarization cocktail was adjusted to 6.7 by addition of hydrochloric acid (HCl) (Roth, Carlsruhe, Germany).

Control cells, termed N0, were cultured in complete medium free of polarizing factors and incubated similarly to N1-like neutrophils. Since neutrophils are prone to spontaneous apoptosis, the experiments were performed in the presence of 3 μM caspase inhibitor Q-VD-OPh (R&D Systems, #OPH001). The different treatments are summarized in **Table 3.1.**

Table 3.1. Treatments for neutrophil polarization

	Substances	**Growth conditions**
N0	Q-VD-OPh	37°C 5% CO_2
N1-like	LPS IFNγ IFNβ Q-VD-OPh	37°C 5% CO_2
N2-like	L-lactate adenosine TGFβ IL-10 PGE_2 G-CSF Q-VD-OPh	37°C 2% O_2 5% CO_2

Q-VD-OPh, Quinoline-Val-Asp-Difluorophenoxymethyl ketone; LPS, Lipopolysaccharide; IFN, Interferon; TGF, Transforming growth factor; PGE_2, prostaglandin E2; IL, interleukin; G-CSF, Granulocyte colony-stimulating factor.

3.3. Preparation of supernatants from colon cancer cells

Supernatants used to test the polarization potential of TLR3-activated colon cancer SW620 cells **(Section 3.4)** were prepared by stimulation of these cancer cells with TLR3 agonist poly(I:C) or medium. Knockdown control cells were prepared through RNA interference (RNAi) and used to verify TLR3-specific induction of polarizing factors.

3.3.1. Principles of RNAi-mediated gene silencing

Experimental RNAi is a fast and easy method for transient gene silencing that exploits the biological pathway of RNAi. The RNAi pathway is naturally present in many eukaryotic cell types where it contributes to viral defense and regulation of gene expression (Hannon, 2002). It depends on the actions of at least two classes of small double stranded RNA (dsRNA) molecules, termed micro RNAs (miRNA)s and small interfering RNAs (siRNA)s, that contribute to gene silencing by neutralizing

complementary mRNA molecules. siRNA exhibits a more specific silencing mechanism than miRNA and is usually the class preferred for gene silencing experiments (Thermo Fischer, 2021).

Such experiments exploit the RNAi pathway by introducing carefully prepared artificial dsRNAs into the host **(Figure 3.2).** Upon arriving in the host cytosol, the artificial RNA "hijacks" the RNAi pathway and is cleaved by the endonuclease Dicer. The cleaved dsRNA then associates with other proteins to form an RNA-induced silencing complex (RISC). Once settled in the RISC, one strand of the siRNA is cleaved off by the endonuclease Argonaute (AGO), leaving one strand of guide RNA to lead the RISC to the target mRNA. Complementary binding between the guide RNA and its target catalyzes a reaction in which AGO cleaves the target mRNA and silencing of the gene of interest is achieved.

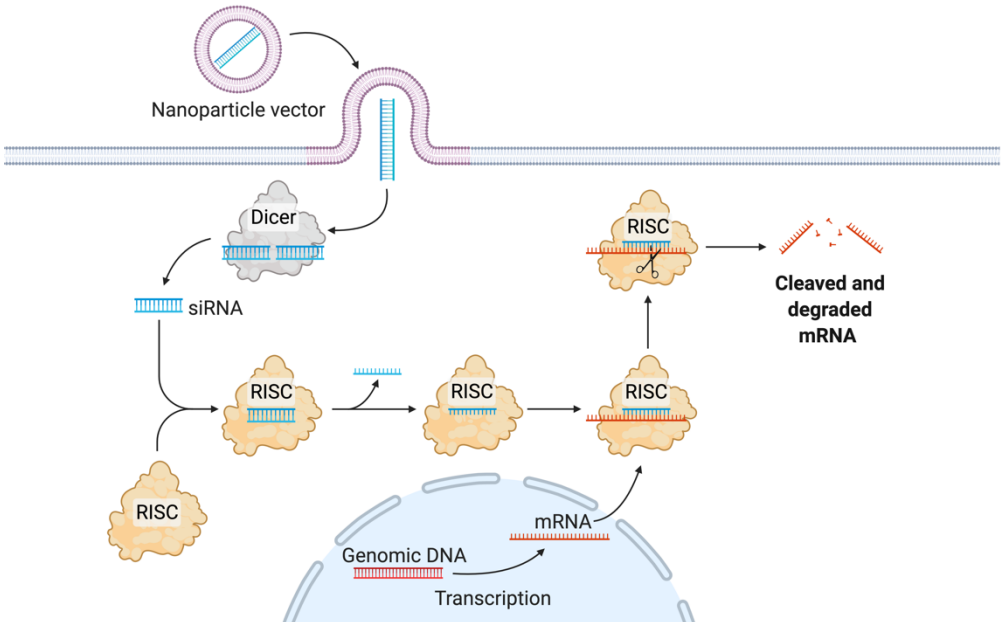

Figure 3.2. Overview of siRNA-mediated RNA interference. *Adapted from BioRender.com*

3.3.2. Sub-culturing procedure

SW620 cells (ATCC) were grown in RPMI 1640 medium supplemented with 2 mM L-Glutamine Solution, 0.05% Gensumycin [Sanofi Aventis, Norway]) and 10% FCS in Corning 75cm^2 Cell Culture Flasks with ventilated caps (Corning Life Sciences, #430641U), and maintained at 37°C in a humidified air atmosphere containing 5% CO2. Subculturing was performed twice a week at 70% confluency as described in **Figure 3.3**, by removing the old medium **(1)**, washing cells with Dulbecco's Phosphate Buffered Saline (DPBS) (Sigma-Aldrich, #D8537) **(2)**, and disrupting adherent proteins with Trypsin/EDTA Solution (Sigma-Aldrich, #T3924) **(3)**. The rate of trypsinization was increased by briefly incubating the cells at 37°C **(4)** before fresh medium was added to neutralize the Trypsin/EDTA Solution **(5)**. A new passage was then established by transferring singularized cells into a new culture flask containing fresh medium **(6)**.

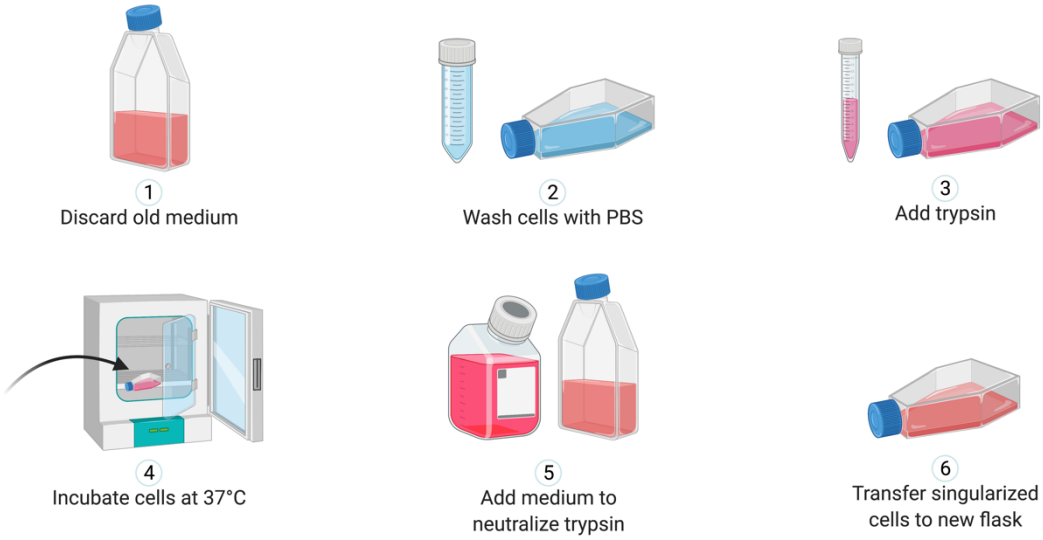

Figure 3.3. Workflow for subculture of adherent cell lines. *Created with BioRender.com*

3.3.3. Silencing of TLR3 and stimulation of cells

Cells were washed once with DPBS and harvested by trypsinization before resuspended in fresh medium (RPMI 1640 supplemented with 2 mM L-Glutamine Solution, 0.05% Gensumycin and 10% FCS) and seeded in Corning 24-well plates (300 000 cells/well at 0.4 mL/well). The seeded cells were rested until the next day or immediately treated with siRNA against TLR3 to silence receptor expression. Silencing was performed by transfecting cells with 10 nM siRNA against TLR3 (Qiagen, #SI02630768) or non-silencing control (Qiagen, #SI03650325) using 20 nM Lipofectamine RNAiMAX (Invitrogen, #13778075). siRNAs were diluted in RPMI 1640 medium before Lipofectamine RNAiMAX was added to create siRNA delivery vectors and the transfection solutions were preincubated for 20 minutes.

The next day, fresh medium was added (RPMI 1640 supplemented with 2 mM L-Glutamine Solution, 0.05% Gensumycin and 2% FCS) and cells were stimulated with 5 μg/mL poly(I:C) (InvivoGen, #vac-pic) or medium. Supernatants from stimulated cells were collected after 24h and stored at -20°C prior to neutrophil polarization experiments. Reduction of TLR3-induced cytokines was verified by enzyme-linked immunosorbent assay (ELISA) and reverse transcription-quantitative polymerase chain reaction (RT-PCR) was performed by Dr. Marit Bugge to confirm target knockdown (data not shown).

3.4. Incubation of neutrophils with supernatants collected from colon cancer cells

Neutrophils were incubated with supernatants collected from poly(I:C)/medium-stimulated SW620 cells to determine if these colon cancer cells release neutrophil-polarizing factors in response to TLR3-activation.

3.4.1. Procedure

Neutrophils were seeded in Corning 24-well plates (4 million cells/mL at 1.875 mL/well) and incubated in N0 medium as described in **Section 3.2.1**. In addition, cells were treated with 250 μL supernatant collected from poly(I:C)/medium stimulated SW620 and knockdown SW620 cells.

3.5. Flow Cytometry of neutrophils

The expression of selected surface markers on freshly isolated and *in vitro* polarized neutrophils was determined by staining with fluorescently conjugated antibodies and multicolor flow cytometry.

3.5.1. Principles of flow cytometry

Flow cytometry is a laser-based technique used to count and profile cells in suspension. It allows for multiparameter analysis of up to thousands of cells per second and is commonly used to measure the expression of cell surface and intracellular molecules, define cell types in heterogenous populations and asses the purity of isolated cell types (Adan et al., 2017).

Once a sample is placed on a flow cytometer instrument it is injected into a flow cell where hydrodynamic focusing is used to force cells to move as single cells towards one or more lasers **(Figure 3.4)**. In this process, a faster-moving salt-based liquid, called sheath fluid, focuses the sample into a smaller core stream, where cells travel along the same axis and at approximately the same rate. As individual cells pass through the laser, they scatter light and emit fluorescence, which is filtered to appropriate signal detectors. The signal detector converts the light signal into an electrical signal that is digitized by the instrument's electronics system and the data associated with each individual cell is binned and stored in a digital format that can be read and analyzed by appropriate computer software.

Signals that were generated from light scattered axial and perpendicular to the laser beam, termed forward scatter (FSC) and side scatter (SSC), can be used to assess a cell's relative size and granularity, whereas fluorescence emitted from fluorescently conjugated antibodies or fluorescent dyes and proteins is used to investigate physiochemical characteristics further.

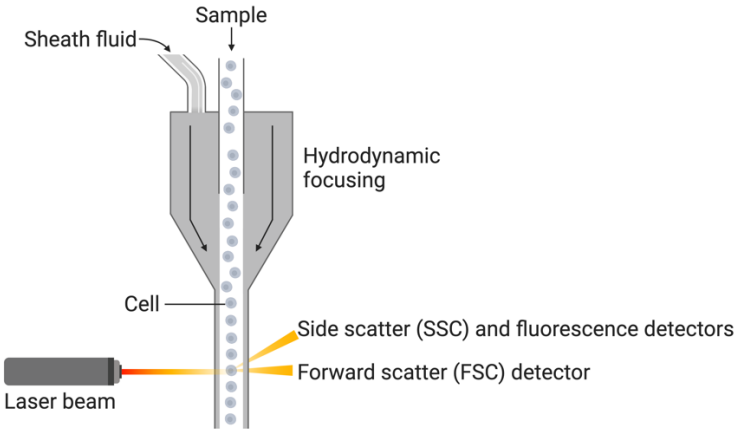

Figure 3.4. Illustration of the flow cytometer flow cell. *Created with BioRender.com*

3.5.2. Optimalization

Staining panels

Antibodies were tested on PBMCs by Dr. Nadra Nilsen and stained the expected populations based on size and granularity (data shown for $CD3^{APC}$, $CD14^{FITC}$, $CD15^{BV605}$ and $CD66b^{BV421}$ in **Figure 4.1**).

Titration of viability dye

The optimal staining concentration for eBioscience Fixable Viability Dye (FVD) eFluor 780 (Invitrogen, #65-0865-14) was determined on monocytic THP-1 cells (ATCC). Cells were resuspended in DPBS to a concentration of 5 million cells/mL and split into two samples. One sample was put on ice, whereas the other was split again before half of the cells were killed with ~70% ethanol (20% of total volume, lab ethanol). The killed cells were washed once with DPBS, spun at 336 x g for 5 minutes at 4°C and resuspended in DPBS before mixed 1:1 with live cells.

Five samples of the live and live:dead populations were distributed onto a Corning 96-well plate (Corning Life Sciences, #3799) and stained with 1 μg/mL, 0.5 μg/mL, 0.25 μg/mL, 0.125 μg/mL and 0 μg/mL of eBioscience FVD eFluor 780 diluted in DPBS in the dark for 10 minutes at 4°C. The stained cells were then transferred to FACS tubes and washed once with and resuspended in FACS buffer (DPBS supplemented with 2% heat-inactivated [HI] Bovine Serum Albumin [BSA] [Sigma-Aldrich, #A7906] and 2% HI human A^+ serum [Department of Immunology and Transfusion Medicine, St. Olavs Hospital, Trondheim]) before analyzed on a BD LSR II (BD) flow cytometer. The optimal staining concentration (0.5 μg/mL) was determined by calculation of the staining index **(Supplementary Figure. 1)**.

Compensation of antibodies and viability dye

Compensation was performed to correct for spillover between fluorescent channels. Antibodies were compensated using OneComp ebeads (Thermo Fisher Scientific, #01-1111-41) and live and dead THP-1 cells stained with 0.5 μg/mL eBioscience FVD eFluor 780 (5 million cells/mL). Single stained bead samples were prepared by staining 1 drop of OneComp ebeads with 1 test of antibody diluted in FACS buffer in the dark at 4°C for 20 minutes. The bead samples were then washed once with FACS buffer, spun at 336 x *g* for 5 min at 4°C and resuspended in fresh buffer. The THP-1 cells were used to set the fluorescence detector voltages for the photomultiplier tubes (PMT)s on the BD LSR II flow cytometer before each single-stained bead sample was run to ensure that positive bead peaks were on-scale. Each bead sample was then run again, and compensation was calculated with the integrated FACSDiva V Software. eBioscience FVD eFluor 780 was compensated similarly using the stained live and dead THP-1 cells to set the negative and positive populations.

3.5.3. Procedure

Neutrophils and reagents were kept on ice during the procedure to limit spontaneous apoptosis. The summarized workflow is given in **Figure 3.5**. Freshly isolated or polarized neutrophils were washed once in DPBS and spun at 336 x g for 10 min at 4°C **(1)**. Acceleration was set to 7 and deceleration to 2 to avoid unwanted activation of cells. The same program was used during all centrifugations. In order to limit non-specific antibody-binding to neutrophil FC-receptors, cells were incubated with 10% FC-block (BD Biosciences, #564220) in FACS buffer for 10 minutes **(2)**.

Neutrophils were stained with antibodies **(Table 3.2)** in FACS buffer in the dark for 20 minutes according to the assembled staining panels **(Table 3.3) (3)**. Staining with Annexin $A5^{FITC}$ (Panel 3) was performed in Annexin A5 binding buffer (Tau Technologies, #A700) due to the calcium-dependency of Annexin A5 binding to phosphatidylserine. To be able to select for live cells during analysis, cells were then washed twice in DPBS **(4)** and incubated with 0.5 μg/mL eBioscience FVD eFluor 780 diluted in DPBS in the dark for 10 minutes **(5)**. Lastly, cells were resuspended in FACS buffer **(6)** and analyzed with compensation on a BD LSR II flow cytometer **(7)**. Data analysis was performed using FlowJo V10.7.1 and the R-based plugin flowAI as described in **Section 3.5.4 (8)**.

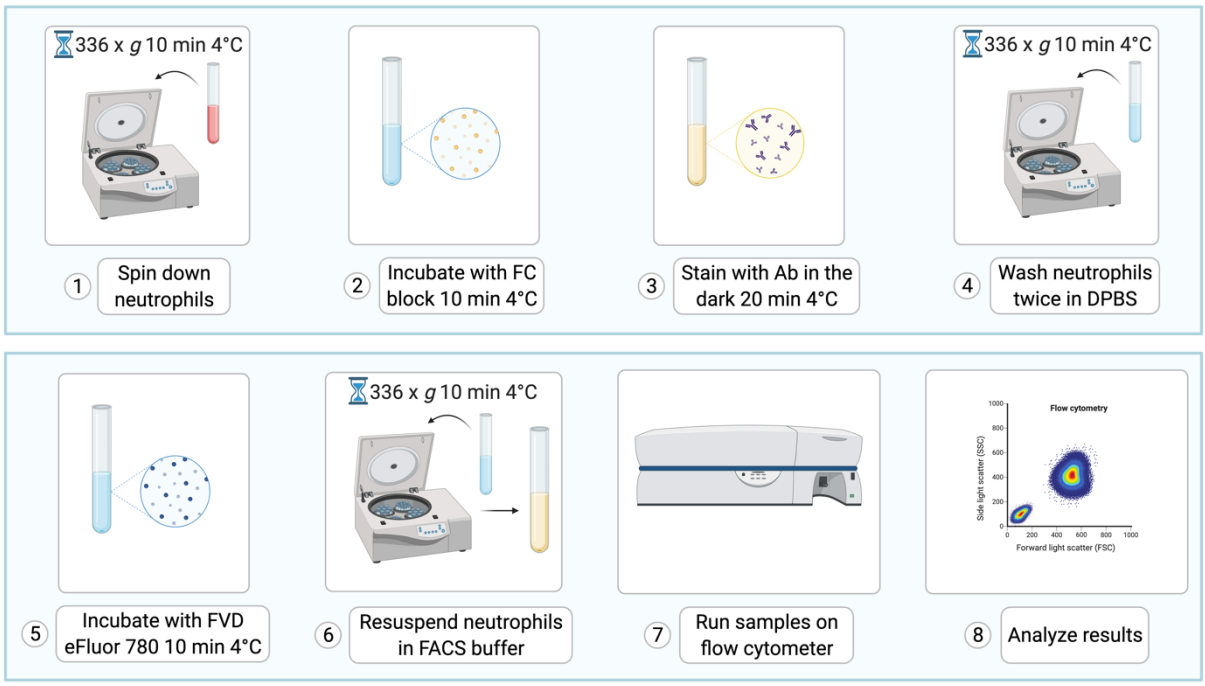

Figure 3.5. Workflow for flow cytometry of neutrophil markers. *Created with BioRender.com*

Table 3.2. Antibodies for flow cytometry

Name	Clone	Isotype	Supplier	Catalog nr.
APC anti-human CD54 Antibody	HA58	Mouse, IgG1, κ	BioLegend	353111
BV421 Mouse Anti-Human CD66b	G10F5	Mouse BALB/c, IgM, κ	BD Horizon	562940
BV605 Mouse Anti-Human CD15	W6D3	Mouse, IgG1, κ	BD Horizon	562980
BV711 Mouse Anti-Human CD95	DX2	Mouse C3H, IgG1, κ	BD Horizon	563132
BV786 Mouse Anti-Human CD62L	SK11	Mouse BALB/c, IgG2a, κ	BD Horizon	565311
CD3 Monoclonal Antibody (OKT3), APC, eBioscience	OKT3	Mouse, IgG2a, κ	Invitrogen	17-0037-42
Annexin A5- FITC	A700	-	Tau Technologies	FI190016
FITC anti-human CD182 (CXCR2) Antibody	5E8/CXCR2	Mouse IgG1, κ	BioLegend	320704
FITC Mouse Anti-human CD14	M5E2	Mouse, IgG2a, κ	BD Biosciences	555397
PE anti-human CD184 (CXCR4) Antibody	12G5	Mouse, IgG2a, κ	BioLegend	306506
PE anti-human CD11b	ICRF44	Mouse IgG1, κ	BioLegend	301306
PE Mouse Anti-Human CD54	HA58	Mouse BALB/c, IgG1, κ	BD Pharmingen	555511
PE Mouse Anti-Human CD19	HIB19	Mouse, IgG1, κ	BD Pharmingen	555413

Table 3.3. Staining panels for flow cytometry

Panel	Antibody	Dilution (/100μL test)	Fluorochrome	Laser	Em. filter
1	BV421 Mouse Anti-Human CD66b	5 μL	BV421	Violet (405 nm)	450/50
	BV605 Mouse Anti-Human CD15	2.5 μL	BV605	Violet (405 nm)	610/20
	CD3 Monoclonal Antibody (OKT3), APC, eBioscience	2.5 μL	APC	Red (640 nm)	670/14
	FITC Mouse Anti-human CD14	5 μL	FITC	Blue (488 nm)	525/50
	PE Mouse Anti-Human CD19	5 μL	PE	Yellow-green (561 nm)	585/20
2	APC anti-human CD54*	2.5 μL	APC	Red (640 nm)	670/14
	BV421 Mouse Anti-Human CD66b	5 μL	BV421	Violet (405 nm)	450/50
	BV605 Mouse Anti-Human CD15	2.5 μL	BV605	Violet (405 nm)	610/20
	BV786 Mouse Anti-Human CD62L	2.5 μL	BV786	Violet (405 nm)	780/60
	FITC anti-human CD182 (CXCR2) Antibody	2.5 μL	FITC	Blue (488 nm)	525/50
	PE anti-human CD11b	2.5 μL	PE	Yellow-green (561 nm)	585/20
3	BV711 Mouse Anti-Human CD95	2.5 μL	BV711	Violet (405 nm)	705/70
	Annexin A5-FITC	2.5 μL	FITC	Blue (488 nm)	525/50
	PE anti-human CD184 (CXCR4)	2.5 μL	PE	Yellow-green (561 nm)	585/20
	PE Mouse Anti-Human CD54*	2.5 μL	PE	Yellow-green (561 nm)	585/20

APC, Allophycocyanin; BV, Brilliant Violet; FITC, fluorescein isothiocyanate; PE, phycoerythrin.

***** Staining against CD54 was performed with either APC anti-human CD54 in panel 2 or PE Mouse Anti-Human CD54 in panel 3. If staining was performed with PE Mouse Anti-Human CD54, PE anti-human CD184 (CXCR4) was not included in the panel.

3.5.4. Data analysis in FlowJo

The analysis of flow cytometry data is built on the principle of gating, which involves drawing a series of outlines called "gates" onto the data plot to select for the population of interest. Data analysis was performed using FlowJo V10.7.1 and the R-based plugin flowAI (Monaco et al., 2016). The data was first cleaned for anomalies by flowAI, which scans for and removes abnormal events caused by unstable flow rate or acquisition related issues **(Figure 3.6)**. Cells were then displayed on eBioscience FVD eFluor 780 and FSC-A properties to select for live cells before FSC-A and SSC-A properties were used to define the main population and remove residual debris **(Figure 4.4)**.

A	**Flow rate** Removal of surges and large deviations of the trend from the median of the flow rate	
B	**Signal acquisition** Removal of acquisition regions whose statistics are shifted from the most stable acquisition region	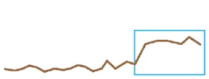
C	**Dynamic range** Removal of outliers in the lower limit and margin events from the upper limit of the dynamic range	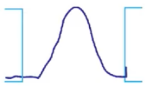

Figure 3.6. The flowAI anomaly discerning tool. flowAI is an R-based quality control plugin for flowJo used to clean flow cytometry files from unwanted events affected by abrupt changes in the flow rate, instability of the signal or limits of the dynamic range of the instrument. The clean-up is performed by anomaly detection algorithms and is conducted in 3 main steps. The first step **(A)** evaluates the steadiness of the flow rate of cells during analysis, which is reconstructed by reporting the number of cells acquired per unit of time. A stable flow rate can be pictured by a line with non-periodic fluctuations but with constant variations, whereas surges and changes in the speed of the fluid (caused by debris or air intrusion into the instrument) represent anomalies. The second step **(B)** verifies the stability of the signal acquisition by plotting fluorescence against time. If cells from a heterogenous population are randomly aspirated in the flow cytometry tube over time, stable acquisition should produce intensity values whose distribution is consistent throughout the analysis. However, technical issues such as defective laser-detection system, voltage instability or poor sample preparation (e.g., lack of vortexing) cause changes in the signal intensities, which are identified as abnormal events. The last step **(C)** checks on recorded signals that fall in the upper or lower limits of the dynamic range and remove events with unacceptable intensity values. *Adapted from (Monaco et al., 2016)*

3.6. Estimation of secreted factors in neutrophil supernatants

Secreted factors in supernatants collected from *in vitro* polarized neutrophils were evaluated by ELISA.

3.6.1. Principles of ELISA

ELISA is an antibody-based technique used to determine and quantify the presence of specific proteins or peptides in a sample. It is considered a gold standard of immunoassays and provides highly sensitive and specific results that are easy to analyze (Aydin, 2015). The method can be performed by different procedures that primarily differ in their strategies for capturing and detecting the target antigen. ELISAs in this project were conducted using DuoSet ELISAs from R&D Systems, which employ a sandwich-based approach for capture and detection (R&D Systems, 2021).

In this approach **(Figure 3.7),** the assay plate is preincubated with a capture antibody and washed to remove unbound material before remaining binding sites are blocked by the addition of a blocking buffer **(1)**. The plate is then rewashed and incubated with samples and standards **(2)**. If the antigen of interest is present in the sample, it specifically binds to the capture antibody. Again, unbound material is removed and a biotinylated detection antibody specific for a different epitope on the antigen is added **(3)**. Addition of this detection antibody leads to the generation of an antigen-antibody complex, which can be detected by successive washes and incubations with a biotin-binding enzyme (streptavidin conjugated to the enzyme horseradish peroxidase [HRP]) and a substrate solution (tetramethylbenzidine [TMB]) **(4)**.

When the HRP enzyme makes contact with the TMB substrate, it catalyzes the oxidation of TMB, turning the solution blue. The intensity of the color is proportional to the amount of HRP activity and can therefore be coupled to the concentration of the target antigen. The color reaction is stabilized with the addition of a sulfuric acid-containing stop solution, resulting in a yellow color **(5)**, and the plate is read at 450 nm **(6)**. A standard curve is calculated using the absorbance values from the standards and used to determine the concentration of the target antigen.

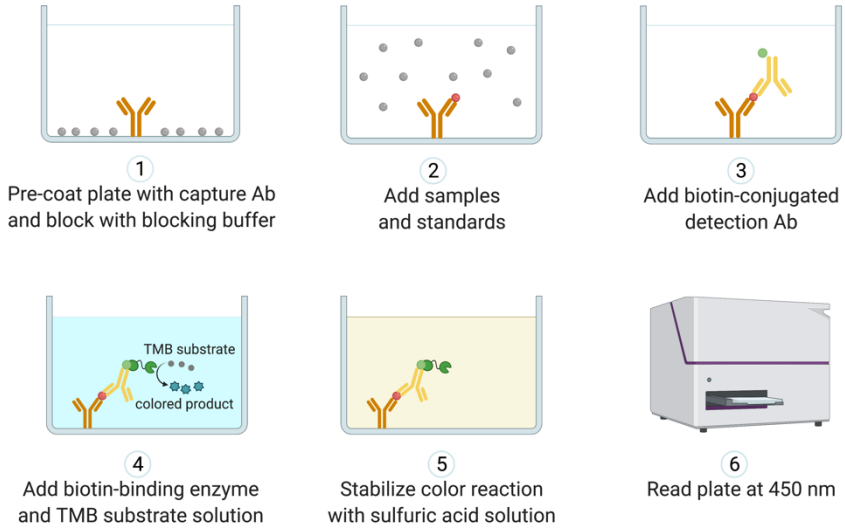

Figure 3.7. Overview of sandwich ELISA. *Created with BioRender.com*

3.6.2. Procedure

Cell supernatants harvested from polarized neutrophils were defrosted at room temperature and analyzed for CXCL10/IP-10 (#DY266), CXCL8/IL-8 (#DY208), TNFa (#DY210), and MPO (#DY317) expression using DuoSet ELISA kits from R&D Systems. The ELISAs were performed in Nunc 96-well plates (Sigma-Aldrich, #M9410) according to the manufacturer's instructions, with the exception of using half of the recommended volumes. Statistical analysis was performed with Prism 9 software using the one-way Analysis of Variance (ANOVA) and Sidak's t-test for multiple comparisons. A p-value < 0.05 was considered statistically significant.

3.7. Gene expression analysis of N1- and N2-like neutrophils

Gene expression analysis of N1- and N2-polarized neutrophils was performed using the NanoString nCounter platform. The experiment was set up by Dr. Marit Bugge.

3.7.1. Principles of the NanoString nCounter platform

The NanoString nCounter platform is a fully automated, amplicon-free technology that quantifies up to 800 RNA, DNA or protein targets in a single run by directly counting the number of target molecules. Using this direct detection strategy, the nCounter enables less hands-on time and provides highly reproducible data (Nanostring, 2021). During analysis, the target of interest is hybridized to specific barcoded capture- and reporter probes **(Figure 3.8)**. After hybridization, the excess probes are removed, before the purified target-probe complexes are immobilized and aligned on an imaging surface. The sample is then scanned by an automated fluorescence microscope, which counts and identifies the labelled barcodes directly before the data is processed by the analysis software.

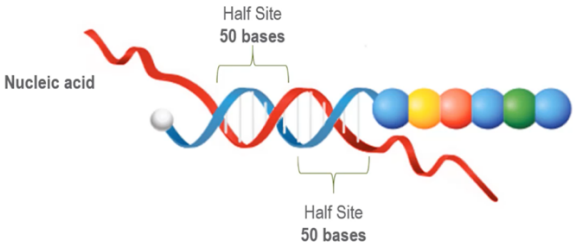

Figure 3.8. Illustration of the nCounter capture and reporter probes. The NanoString nCounter platform employs two oligonucleotide probes to identify and count target molecules. Both probes contain a hybridization region of approximately 50 nucleotides that is specific for the target of interest. In addition, the capture probe contains a biotin molecule at the end, which immobilizes the target onto a streptavidin-coated imaging surface and the reporter probe contains a 6-spot fluorescent barcode that is unique for each target. *Adapted from Nanostring, 2021.*

3.7.2. Isolation of RNA

RNA was isolated from neutrophils using the RNAeasy Mini Kit from Qiagen (#74104) according to the manufacturer's instructions.

3.7.3. Gene expression analysis

RNA was isolated from neutrophils as described in **Section 3.7.2**. Gene expression analysis was performed on the NanoString nCounter platform using the nCounter PanCancer Immune Profiling Panel (NanoString, #XT-CSO-HIP1-12), which contains 730 cancer-related human genes + 40 internal reference genes. The procedure was performed according to the manufacturer's instructions, applying ~100 ng mRNA. Data analysis was performed using nSolver V4.0 and the Advanced Analysis 2.0 plugin.

4. Results

4.1. Primary human neutrophils can be polarized toward N1- and N2-like phenotypes *in vitro*

Immune cells are often polarized in responses associated with infection, inflammation, tissue damage and tumorigenesis. During this process they take on distinct activation states and gain the ability to perform specialized functions in response to specific signals. It is recognized that immune cells play key roles in tumor progression and neutrophils constitute a significant portion of the immune cell types infiltrating the TME (Anderson and Simon, 2020). Inside the TME, a number of molecular signals can promote neutrophil polarization into opposite phenotypes of antitumorigenic (N1) and pro-tumorigenic (N2) TANs (Fridlender et al., 2009). To date, most studies on this dual role in tumorigenesis has been based on murine models, but a promising new method for generating N1- and N2-like neutrophils *in vitro* was recently reported by Mareike Ohms et al. (Ohms et al., 2020).

In order to assess this newly developed method, primary human neutrophils were isolated from healthy blood donors and subjected to *in vitro* polarization based on the protocol by Ohms et al. (Ohms et al., 2020). The N1- and N2-polarized cells were assayed by staining with fluorescently conjugated antibodies and flow cytometry to determine their expression of selected surface markers. In addition, supernatants were collected from the polarized cells and analyzed by ELISA to investigate their secretion of selected soluble factors.

4.1.1. Purity assessment of freshly isolated neutrophils

The purity of freshly isolated neutrophils was assessed by surface antibody staining and flow cytometry against granulocyte markers CD15 and CD66b. Cells were also stained with antibodies against the T-cell marker CD3 and the monocyte marker CD14 to identify contaminating T-cell or monocyte populations. Live cells were selected for based on viability dye staining with eBioscience FVD eFluor 780.

Testing antibodies on PBMCs

The antibodies were initially tested on peripheral mononuclear cells (PBMC)s isolated from healthy donor blood. **Figure 4.1A** shows forward- (FSC-A) and side scatter (SSC-A), and gating of PBMCs. Surface staining of PBMCs revealed a population of cells (~54% of PBMCs) that stained strongly for CD3 and were negative for CD15 **(Figure 4.1B)**. Back-gating onto scatter properties indicated that these cells were T-cells and that the CD3 antibody could detect these cells. Dual staining of PBMCs for CD14 and CD15 **(Figure 4.1C)** revealed a population (~23% of PBMCs) that stained positively for CD14 but displayed varying expression of CD15. Back-gating onto scatter properties indicated that these cells

were monocytes, which in accordance with previous reports express varying levels of CD15 (Lambert et al., 2017).

PBMCs may contain some granulocytes due to insufficient separation, but there was no clear third population above the T-cell population in the FSC-A vs SSC-A plot **(Figure 4.1A)**, indicating that few granulocytes were present. Staining of PBMCs against CD15 and CD66b showed that PBMCs were negative for CD66b, but that a proportion of cells stained positively for CD15 (~24% of PBMCs). Back-gating onto scatter properties of this population indicated that these cells were monocytes **(Figure 4.1C)**. The results suggest that a fraction of PBMCs which is likely monocytes display some expression of CD15, but not CD66b and that CD66b may be a better marker for neutrophils if the antibody stains these cells. Both CD66b and CD15 were used in combination in the following experiments to determine neutrophil purity, since CD15 expression is reported to be much higher in neutrophils.

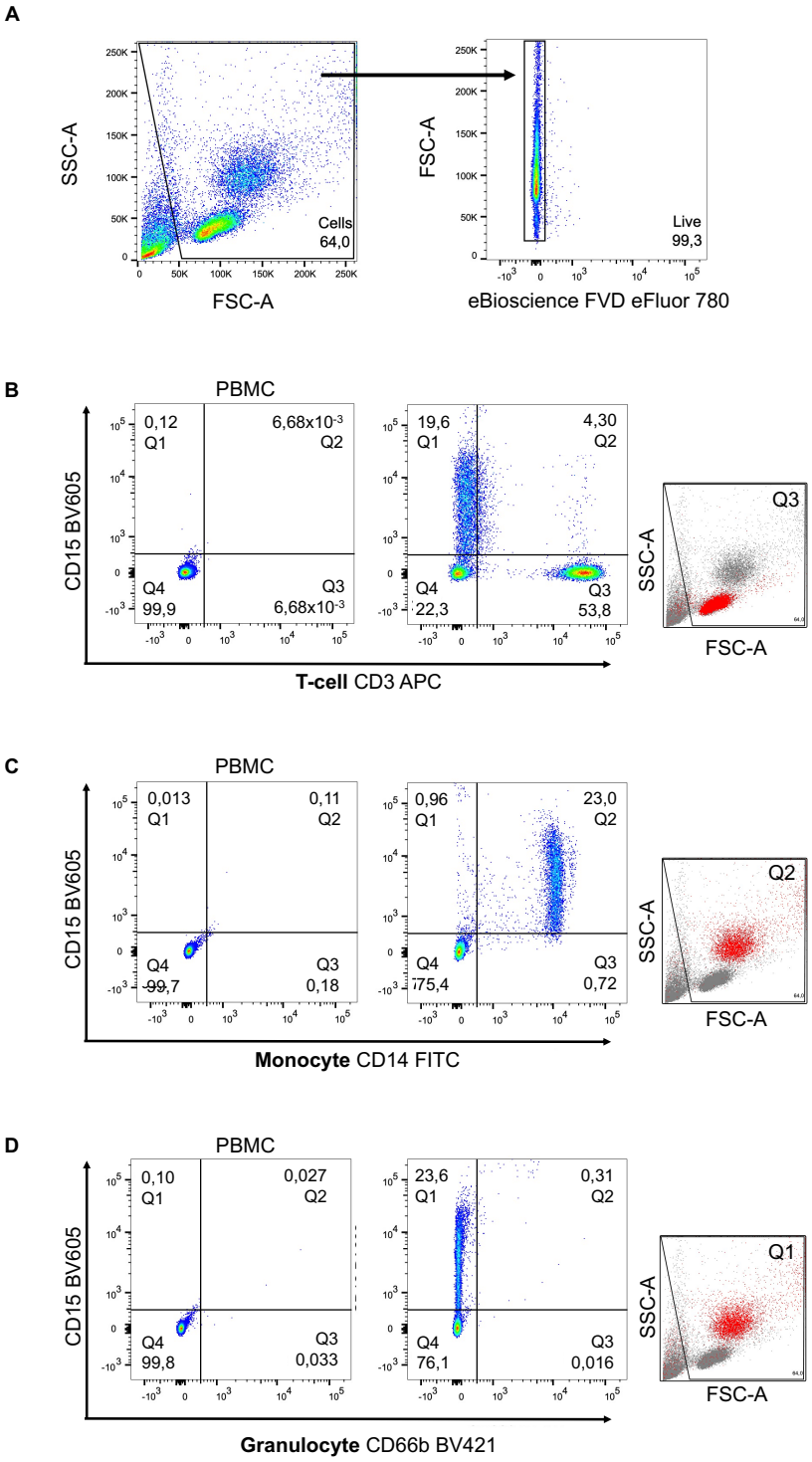

Figure 4.1. A population in PBMCs resembling monocytes stains positively for CD14 and CD15 but not CD66b. Human peripheral mononuclear cells (PBMC)s isolated from a healthy blood donor were stained with antibodies and eBioscience FVD eFluor 780, and analyzed with compensation on a BD LSR II flow cytometer (BD). Cells were gated to remove debris (FSC-A/SSC-A) and dead cells (eBioscience FVD eFluor 780/FSC-A) **(A)**. An unstained control was used to set the quadrants and defined single positive cells (Q1 and Q3), double positive cells (Q2) and double negative cells (Q4). Bivariate plots show staining against T-cells **(B)**, monocytes **(C)** and granulocytes **(D)** and back-gating of positive populations onto scatter properties (FSC-A/SSC-A). Numbers in gates represent frequencies.

Determination of neutrophil purity

Freshly isolated neutrophils from two healthy donors were assessed for purity against T-cells and monocytes using the antibodies tested in **Figure 4.1**. FSC-A and SSC-A, and gating strategy is shown in **Figure 4.2A**. Dual staining with CD15 and CD66b antibodies revealed two populations of $CD15^{+}CD66b^{+}$ cells **(Figure 4.2B)**. A population with intermediate expression of CD15 and high expression of CD66b was observed for both donors (indicated by red gates). These populations represented ~5-10% of the total CD66b positive cells and back-gating onto scatter properties revealed that these were more granular (increased SSC-A) than the cells in the main populations (indicated by green gates) **(Figure 4.2C)**.

Based on the high degree of granularity (Gopinath and Nutman, 1997), intermediate CD15 expression (Lecot et al., 2019, Bochner et al., 1994) and high CD66b expression (Yoon et al., 2007), these cells were believed to be eosinophils, a type of granulocyte involved in allergic reactions and host defense against parasites. Since the nature of these cells were unclear and represented only a small portion of the total cell population (~5-10%), this population was gated away in the following analyses **(Figure 4.4)**. Less than 1% of cells stained positively for T-cell CD3 (~0% of cells) **(Figure 4.2D)** and monocyte CD14 (~0.2-0.5% of cells) **(Figure 4.2E)**, indicating that very few T-cells or monocytes contaminated the isolated neutrophils. Combined, these results indicate neutrophil populations with ~88-93% purity.

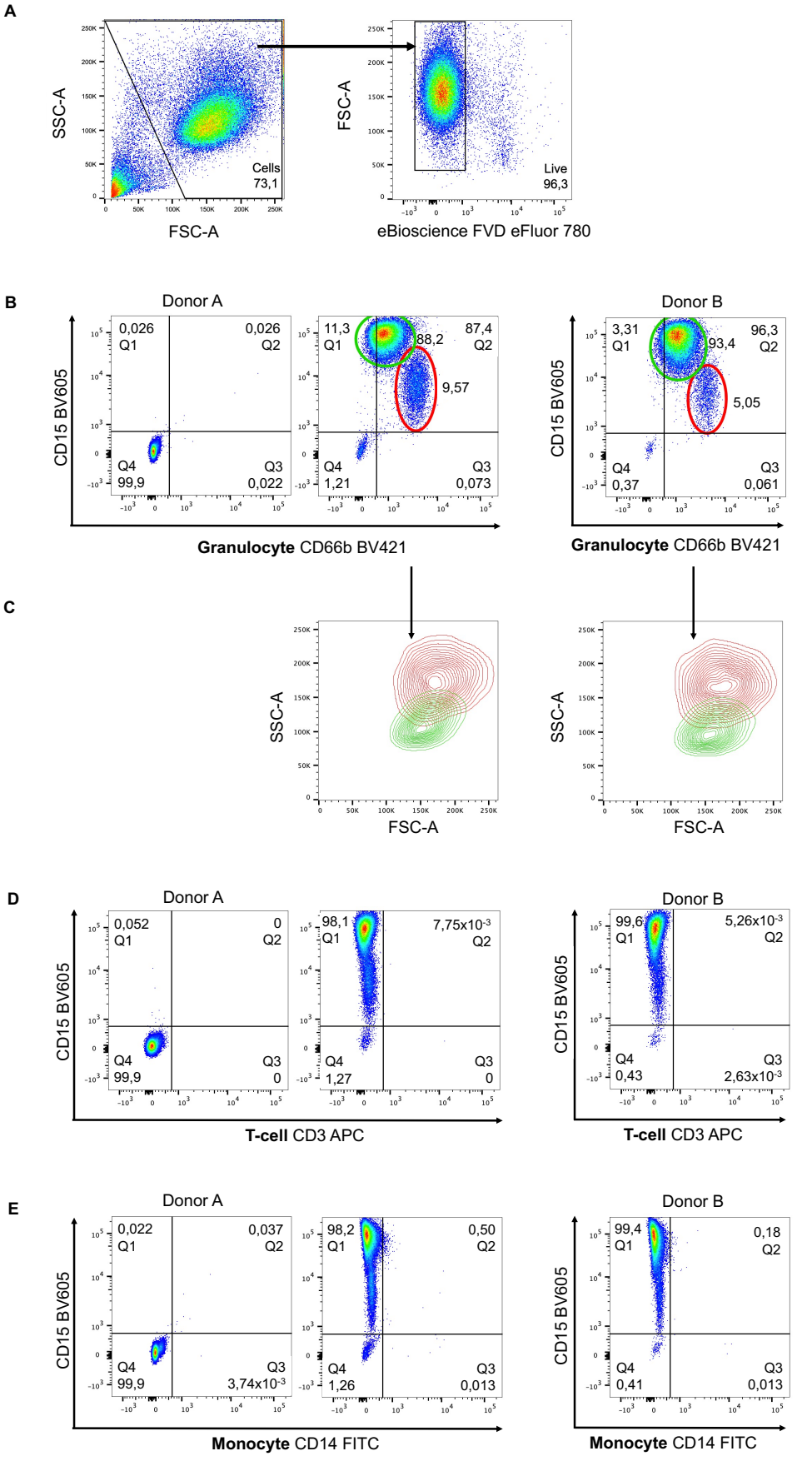
A
SSC-A
FSC-A
Cells
73,1
FSC-A
eBioscience FVD eFluor 780
Live
96,3
B
Donor A
Donor B
CD15 BV605
Granulocyte CD66b BV421
0,026
Q1
0,026
Q2
Q4
99,9
Q3
0,022
11,3
Q1
88,2
87,4
Q2
9,57
Q4
1,21
Q3
0,073
3,31
Q1
93,4
96,3
Q2
5,05
Q4
0,37
Q3
0,061
C
SSC-A
FSC-A
D
Donor A
Donor B
CD15 BV605
T-cell CD3 APC
0,052
Q1
0
Q2
Q4
99,9
Q3
0
98,1
Q1
7,75x10-3
Q2
Q4
1,27
Q3
0
99,6
Q1
5,26x10-3
Q2
Q4
0,43
Q3
2,63x10-3
E
Donor A
Donor B
CD15 BV605
Monocyte CD14 FITC
0,022
Q1
0,037
Q2
Q4
99,9
Q3
3,74x10-3
98,2
Q1
0,50
Q2
Q4
1,26
Q3
0,013
99,4
Q1
0,18
Q2
Q4
0,41
Q3
0,013

Figure 4.2. Purity assessment of isolated neutrophils. Primary human neutrophils were isolated from two healthy blood donors, stained with antibodies and eBioscience FVD eFluor 780, and analyzed with compensation on a BD LSR II flow cytometer (BD). The data was gated to remove debris (FSC-A/SSC-A) and dead cells (eBioscience FVD eFluor 780/FSC-A) **(A)**. An unstained control from Donor A was used to set the quadrants and defined single positive cells (Q1 and Q3), double positive cells (Q2) and double negative cells (Q4). Bivariate plots show neutrophil purity assessed against granulocyte CD66b **(B)** T-cell CD3 **(D)** and monocyte CD14 **(E)**. Overlaid contour plots show back-gating of intermediate $CD15^+$ and high $CD66b^+$ cells observed in B **(C)**. Numbers in or adjacent to gates represent frequencies.

4.1.2. *In vitro* polarized neutrophils express markers typical of N1 and N2 TANs

Freshly isolated neutrophils were subjected to *in vitro* polarization to generate N1- and N2-like cells. Polarization was performed for 24- and 48h in the presence of an N1-polarization cocktail containing proinflammatory mediators or an N2-polarization cocktail mimicking hallmarks of the TME (Ohms et al., 2020). N1-polarization was accordingly performed in the presence of LPS, IFNγ and IFNβ at 37°C and 5% CO_2, whereas N2-polarization was conducted in hypoxic conditions (2% O_2, 5% CO_2, 37°C) in the presence of L-lactate, adenosine, TGFβ, IL-10, PGE_2 and G-CSF (**Figure 4.3**). N0 control cells were cultured in medium free of polarizing factors and incubated similar to N1-like neutrophils. Since neutrophils are prone to spontaneous apoptosis, the experiments were performed in the presence of a caspase inhibitor.

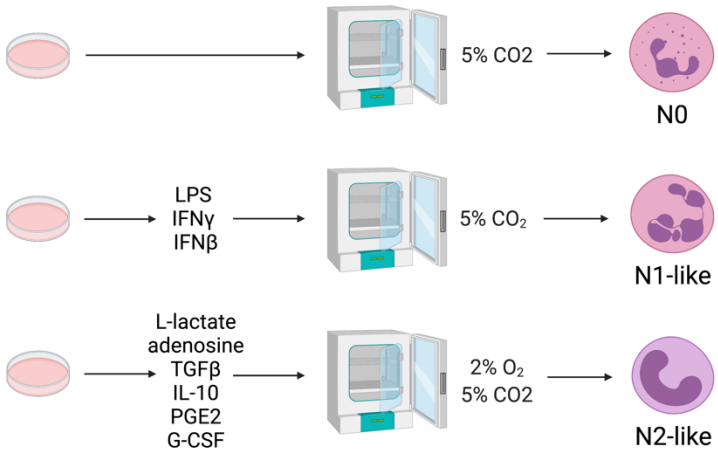

Figure 4.3. Illustration of the Ohms et al. method for generating N0, N1-like and N2-like TANs. Primary human neutrophils were isolated from healthy blood donors. N1-like neutrophils were generated through incubation with a polarization cocktail containing lipopolysaccharide (LPS) (100 ng/mL), interferon gamma (IFNγ) (50 ng/mL) and interferon beta (IFNβ) (10.000 U/mL) at 37°C and 5% CO_2. Ohms et al. reported the bacterial endotoxin LPS as an activator of neutrophil functions and the cytokines IFNγ and IFNβ as inducers of N1 tumor-associated neutrophils (TAN)s (Gomes et al., 2010, Ellis and Beaman, 2004, Andzinski et al., 2016). N2-like neutrophils were generated through incubation with a polarization cocktail composed of L-lactate (25 mM), adenosine (10 μM), transforming growth factor beta (TGFβ) (20 ng/mL), interleukin-10 (IL-10) (10 ng/mL), prostaglandin E_2 (PGE_2) (20 ng/mL) and granulocyte colony-stimulating factor (G-CSF) (100 ng/mL) at 37°C with 2% O_2 and 5% CO_2. Ohms et al. described TGFβ, IL-10, PGE_2 and G-CSF as inducers of N2 TANs in *in vivo* studies and high levels of L-lactate and adenosine as characteristic of the tumor microenvironment (TME) (Fridlender et al., 2009, Gerlini et al., 2004, Greenhough et al., 2009, Chakraborty and Guha, 2007, Romero-Garcia et al., 2016, Leone and Emens, 2018). N0 control cells were cultured in medium free of polarizing factors and incubated similar to N1-like neutrophils. Because neutrophils are prone to spontaneous apoptosis, the experiments were performed in the presence of the caspase inhibitor Q-VD-OPh (3μM). *Created with BioRender.com*

In vitro polarized neutrophils from two donors were harvested at 24- and 48h and subjected to antibody staining and flow cytometry against markers described for *in vivo* N1- and N2 TANs. Based on studies of TANs from murine tumor models, Ohms et al. defined the adhesion molecule CD54/ICAM-1 and the cell death receptor CD95/Fas as markers of the antitumorigenic N1 phenotype (Fridlender and Albelda, 2012), and the chemokine CXCR2 as a marker for the pro-tumorigenic N2 state (Chao et al., 2016, Nywening et al., 2018). The resulting data was gated using a 2-step approach to exclude dead cells and debris from the analysis **(Figure 4.4)**, in addition to the population of unclear nature identified during purity assessment **(Figure 4.2A-B)**. The ungated cell population **(A)** was displayed on eBioscience FVD eFluor 780 and FSC-A properties **(B)** and dead cells were excluded by drawing a gate around eBioscience FVD eFluor 780 negative cells. The fraction of live cells was then displayed on FSC-A and SSC-A and a gate was drawn around the main population **(C)**. The same gating was used in all flow cytometry analyses.

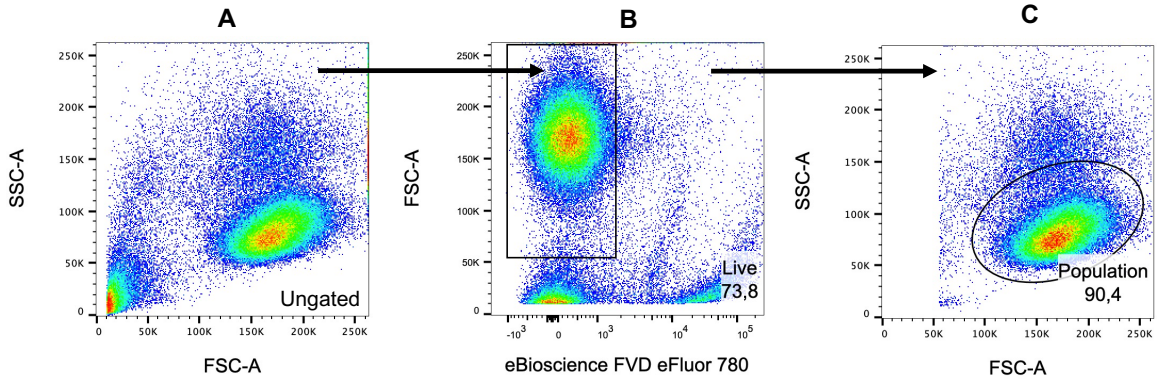

Figure 4.4. Representative gating strategy for the analysis of flow cytometry data. Flow cytometry data was gated by a two-step approach to remove dead cells and debris from the analysis, and to define the cells of interest. Ungated cells **(A)** were displayed on eBioscience FVD eFluor 780 and FSC-A properties **(B)** to select for live cells. The fraction of live cells was then displayed on FSC-A and SSC-A to define the cells of interest **(C)**. Numbers in gates represent cell frequencies.

The expression of each phenotypic marker on freshly isolated, non-polarized neutrophils is shown in **Figure 4.5A** and demonstrate low background staining with $CXCR2^{FITC}$, $CD95^{BV711}$ and $CD54^{APC}$ antibodies. The characterization of these markers on *in vitro* polarized neutrophils revealed a prominent increase in surface CD95 and CD54 on cells cultured in the presence of the N1-polarization cocktail **(Figure 4.5C-D)**. In contrast, the expression of CXCR2 was downregulated on these cells compared to the N0 control **(Figure 4.5B)**. Neutrophils that were cultured in the presence of the N2 polarization cocktail displayed similar levels of CD95 and CD54 to N0 control cells **(Figure 4.5C-D),** whereas the expression of CXCR2 was highly upregulated **(Figure 4.5B)**. These results indicate that *in vitro* polarized N1-like cells upregulate their expression of CD54 and CD95 and downregulate their expression of CXCR2. In contrast, N2-polarized cells express similar levels of CD54 and CD95 to nonpolarized neutrophils but upregulate their expression of CXCR2.

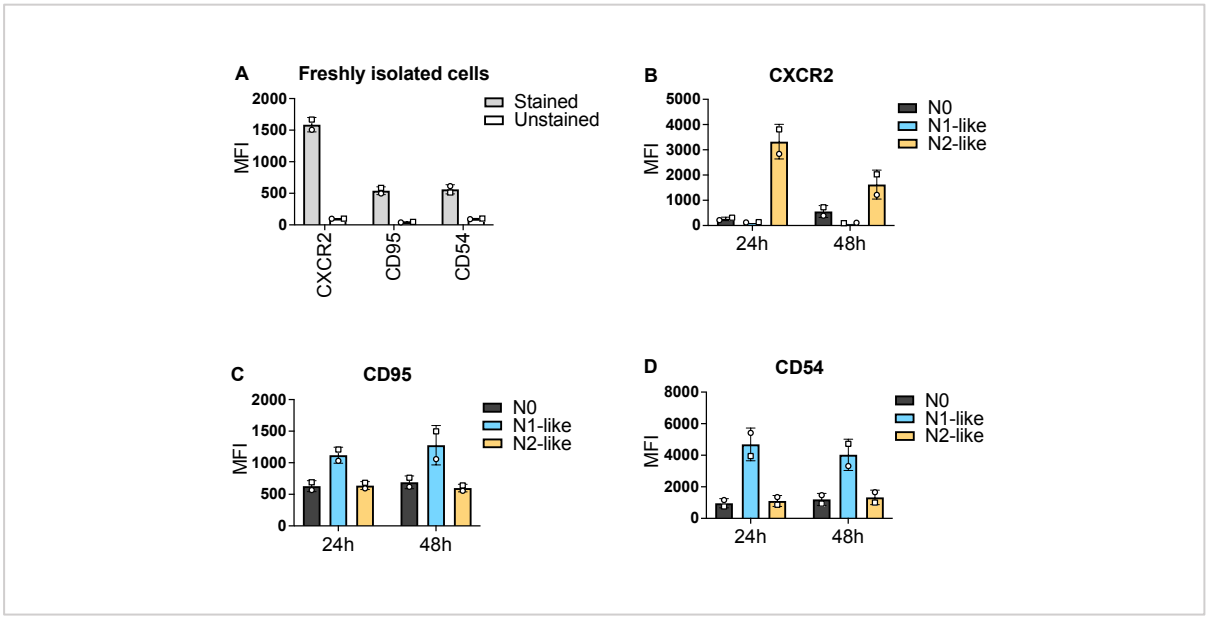

Figure 4.5. Expression of CXCR2, CD95 and CD54 on *in vitro* polarized neutrophils. Primary human neutrophils isolated from two healthy blood donors were subjected to *in vitro* polarization based on a protocol by Mareike Ohms et al. (Ohms et al., 2020). N1- and N2-like cells were cultured in the presence of an N1- or N2 polarization cocktail containing caspase inhibitor Q-VD-OPh, whereas N0 control cells were treated with Q-VD-OPh only. N1-like and N0 cells were incubated at 37°C in a humidified air atmosphere containing 5% CO_2, whereas N2-like cells were incubated in a humidified hypoxic chamber at 37°C with 2% O_2 and 5% CO_2. Cells were assayed at 0h **(A)** and at 24- and 48h for their expression of surface CXCR2 **(B)**, CD95/Fas **(C)** and CD54/ICAM-1 **(D)** by staining with antibodies and flow cytometry. The analysis was performed with compensation on a BD LSR II flow cytometer (BD). Bar plots show median fluorescence intensity (MFI) ± SD (n=2) with donor A data presented as circles and Donor B data indicated by squares. Flow cytometry data was gated as described in **Figure 4.4**.

4.1.3. N1-like neutrophils exhibit an activated phenotype compared to N2-like neutrophils

Next, the activation status of *in vitro* polarized N1- and N2-like neutrophils from two donors was assessed by antibody staining and flow cytometry against the activation marker CD62L (L-selectin) and degranulation markers CD66b/CEACAM8 and CD11b/integrin alpha M. CD62L is a cell adhesion molecule involved in neutrophil migration across the endothelium. It is rapidly shed from the cell surface upon contact with neutrophil activating ligands (Ivetic, 2018) and was used as a marker to distinguish non-activated $CD62L^{high}$ neutrophils from activated $CD62L^{low}$ neutrophils (Ohms et al., 2020). The adhesion receptors CD66b and CD11b are usually present in the membranes of neutrophil granules (Ducker and Skubitz, 1992, Sengelov et al., 1993). Because the granule membrane fuses with the plasma membrane upon granule release, these adhesion molecules were used as markers to determine neutrophil degranulation (Ohms et al., 2020).

The expression of each marker on freshly isolated, non-polarized neutrophils is shown in **Figure 4.6A** and demonstrate low background staining with CD62L^{BV786}, CD11b^{PE} and CD66b^{BV421}. The data revealed that N1-polarized and N0 control cells display increased shedding of CD62L compared to N2-polarized neutrophils **(Figure 4.6B)**. Further, the expression of degranulation markers CD11b and CD66b were greater on N1-like neutrophils compared to N2-polarized and N0 cells **(Figure 4.6C-D)**, which indicates an activated status for N1-like neutrophils compared to N2-like neutrophils.

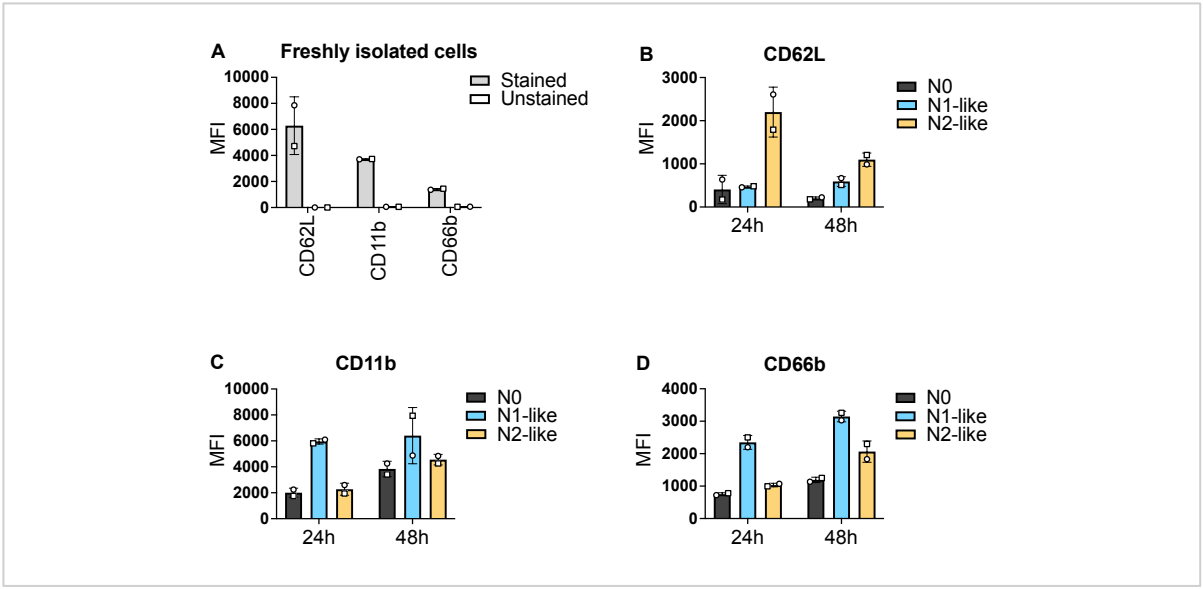

Figure 4.6. Expression of CD62L, CD11b and CD66b on *in vitro* polarized neutrophils. Primary human neutrophils isolated from two healthy blood donors were subjected to *in vitro* polarization based on a protocol by Mareike Ohms et al. (Ohms et al., 2020). N1- and N2-like cells were cultured in the presence of an N1- or N2 polarization cocktail containing caspase inhibitor Q-VD-OPh, whereas N0 control cells were treated with Q-VD-OPh only. N1-like and N0 cells were incubated at 37°C in a humidified air atmosphere containing 5% CO_2, whereas N2-like cells were incubated in a humidified hypoxic chamber at 37°C with 2% O_2 and 5% CO_2. Cells were assayed at 0h **(A)** and at 24- and 48h for their expression of surface CD62L/L-selectin **(B)**, CD11b/integrin alpha M **(C)** and CD66b/CEACAM8 **(D)** by staining with antibodies and flow cytometry. The analysis was performed with compensation on a BD LSR II flow cytometer (BD). Bar plots show median fluorescence intensity (MFI) ± SD (n=2) with donor A data presented as circles and Donor B data indicated by squares. Flow cytometry data was gated as described in **Figure 4.4**.

4.1.4. *In vitro* polarized neutrophils secrete factors typical of N1 and N2 TANs

Supernatants were collected from *in vitro* polarized neutrophils from four donors at 24- and 48h to investigate the secretion profiles of these cells. Ohms et al. reported increased production of the proinflammatory cytokines CXCL10/IP10, TNFα and the ROS-generating enzyme myeloperoxidase (MPO) for N1 neutrophils (Fridlender and Albelda, 2012) and high secretion of the neutrophil-attracting

chemokine CXCL8/IL-8 for N2 neutrophils (Fridlender et al., 2009). The supernatants were accordingly assayed by ELISA for the presence of these mediators.

The results showed that neutrophils grown in the presence of the N1-polarization cocktail displayed the highest secretion of all four markers. Compared to the N0 control, a significant induction of CXCL10 and MPO could be observed after only 24h **(Figure 4.7A-B)**, whereas TNFα and CXCL8 production was observed at the 48h timepoint only **(Figure 4.7C-D)**. N2-polarized cells did not secrete CXCL10 or TNFα **(Figure 4.7A&C)**. These cells released low levels of MPO at 24- and 48h, similar to N0 control cells, whereas CXCL8 secretion was only observed at the 48h timepoint. However, the production of MPO and CXCL8 at 48h was not significant. These findings suggest that proinflammatory CXCL10, MPO, TNFα and CXCL8 are induced in N1-like neutrophils and that CXCL8 might be induced in N2-like neutrophils.

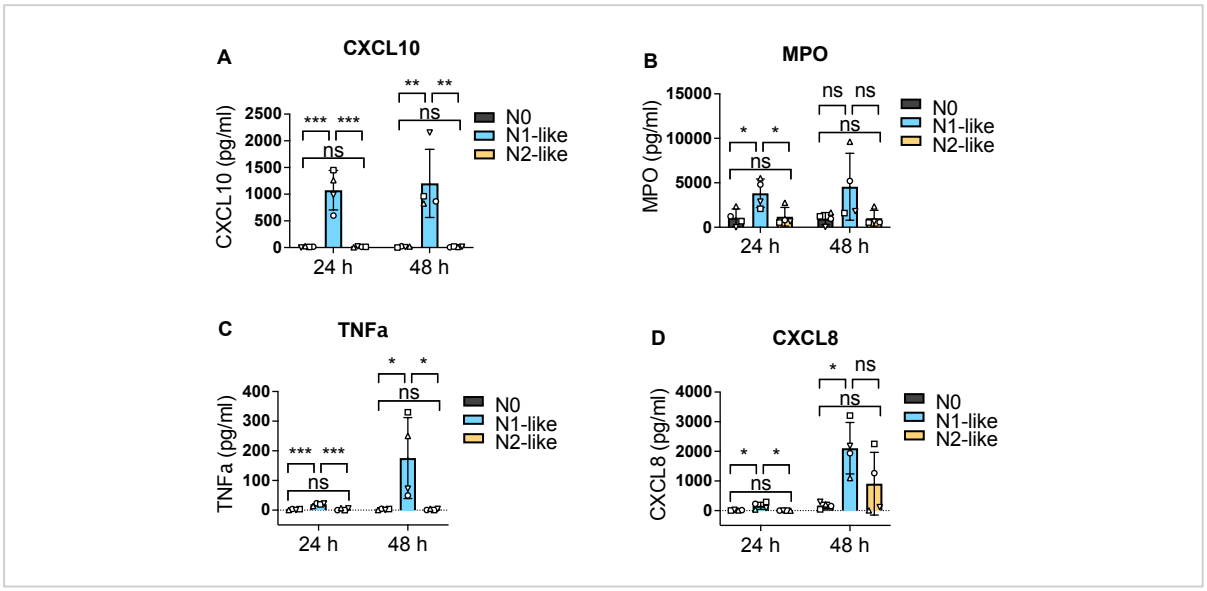

Figure 4.7. Secretion of TNFα, CXCL10 and CXCL8 by *in vitro* polarized neutrophils. Primary human neutrophils isolated from four healthy blood donors were subjected to *in vitro* polarization based on a protocol by Mareike Ohms et al. (Ohms et al., 2020). N1- and N2-like cells were cultured in the presence of an N1- or N2 polarization cocktail containing caspase inhibitor Q-VD-OPh, whereas N0 control cells were treated with Q-VD-OPh only. N1-like and N0 cells were incubated at 37°C in a humidified air atmosphere containing 5% CO_2, whereas N2-like cells were incubated in a humidified hypoxic chamber at 37°C with 2% O_2 and 5% CO_2. Supernatants were harvested at 24- and 48h and assayed by ELISA for CXCL10/IP-10 **(A)**, TNFα **(B)**, CXCL8/IL-8 **(C)** and MPO **(D)**. Bar plots show concentration (pg/mL) ± SD (n=4). Each donor is represented by individual symbol shapes. P-values were calculated with one-way ANOVA and Sidak's t-test for multiple comparisons. *p < 0.05, **p < 0.01, ***p < 0.001, ns = not significant.

4.1.5. Viability of neutrophils after 24- and 48h polarization

The viability of N1- and N2-like cells at 24- and 48h was determined by flow cytometry of cells stained with Annexin $A5^{FITC}$ and eBioscience FVD eFluor 780. Annexin A5 binds with high affinity to phosphatidylserine, a phospholipid that is translocated to the outer leaflet of the plasma membrane during apoptosis. Fluorescently conjugated Annexin A5 is therefore frequently used in flow cytometry to detect apoptotic cells. Viability dyes such as eBioscience FVD eFluor 780 are protein-binding dyes used to label dead cells. These dyes only bind to the cell surface in living cells, resulting in a very dim fluorescence but stain with bright fluorescence in dead cells, which have compromised membranes.

The flow cytometry data was gated using a 3-step strategy **(Figure 4.8)** to exclude cell fragments and debris from the analysis. Debris events typically end up in the live fraction of cells and are important to remove to avoid misleading results. Cells were displayed on Annexin $A5^{FITC}$ and eBioscience FVD eFluor 780 to define double-negative events **(4.8A)**. The double-negative region was displayed on scatter properties and the subset of events with very low FSC-A was defined as debris. The debris gate was then inverted to remove these events from the analysis **(4.8B)**. Finally, the inverted gate was added to the ungated population **(4.8C)**.

The gated data was displayed on Annexin $A5^{FITC}$ and eBioscience FVD eFluor 780 to determine the percentage of viable cells **(4.8D)**. Quadrant 1 (Q1) represented negative Annexin $A5^{FITC}$ and positive eBioscience FVD eFluor 780 staining and indicated necrosis. Q2 represented double-positive staining and indicated late apoptosis. Q3 represented positive Annexin $A5^{FITC}$ and negative eBioscience FVD eFluor 780 staining and indicated early apoptosis. Q4 represented double-negative staining and indicated viable cells. The percentages of viable cells for N0, N1-like and N2-like neutrophils are summarized in **Figure 4.9**. The results indicate that compared to the N0 control, the polarization treatments did not have notable impacts on viability during the first 24h **(A)**. However, between 24- and 48h **(B)** the percentage of viable cells decreased from ~80% to ~55% in cultures treated with the N1- or N2-polarization cocktails.

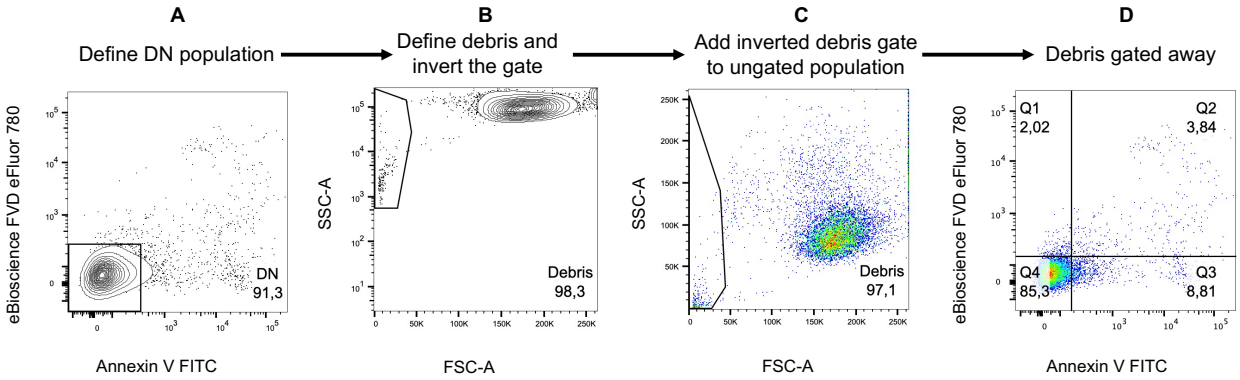

Figure 4.8. Representative gating strategy for assessment of cell death. Flow cytometry data for assessment of cell death was gated using a three-step approach to remove cell fragments and debris events. Double-negative (DN) events were defined on Annexin A5^{FITC} and eBioscience FVD eFluor 780 **(A)**. DN events were then displayed on FSC-A/SSC-A and low FSC-A events were defined as debris **(B)**. The debris gate was inverted and added to the ungated population **(C)**. The gated data was displayed on Annexin A5^{FITC} and eBioscience FVD eFluor 780 **(D)**. Quadrants indicate necrotic- (Q1), late apoptotic- (Q2), early apoptotic- (Q3) and viable cells (Q4). Numbers in or adjacent to gates represent frequencies.

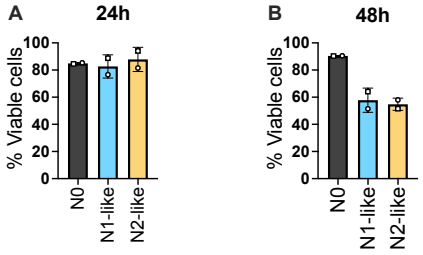

Figure 4.9. Percentage of viable cells at 24- and 48h. Primary human neutrophils were isolated from two healthy blood donors and subjected to *in vitro* polarization based on a protocol developed by Mareike Ohms et al. (Ohms et al., 2020). N1- and N2-like cells were cultured in the presence of an N1- or N2 polarization cocktail containing caspase inhibitor Q-VD-OPh, whereas N0 control cells were treated with Q-VD-OPh only. N1-like and N0 cells were incubated at 37°C in a humidified air atmosphere containing 5% CO_2, whereas N2-like cells were incubated in a humidified hypoxic chamber at 37°C with 2% O_2 and 5% CO_2. Cells were harvested at 24- and 48h, stained with Annexin A5^{FITC} and eBioscience FVD eFluor 780, and analyzed with compensation on a BD LSR II flow cytometer (BD). The data was gated as described in **Figure 4.8**. Bar plots show the percentage of cells double-negative for Annexin A5^{FITC} and eBioscience FVD eFluor 780 at 24h **(A)** and 48h **(B)** ± SD (n=2). Donor A data are presented as circles and Donor B data are indicated by squares.

4.2. *In vitro* polarized neutrophils exhibit distinct transcriptional profiles

The active and dynamic neutrophil response towards infection or inflammation is associated with changes in gene expression (Newburger et al., 2000). In order to characterize the N1- and N2-like neutrophils generated from *in vitro* polarization, the transcriptomic changes underlying these opposite activation states was investigated by differential gene expression analysis. RNA was isolated from N1- and N2-polarized cells from two donors and compared to non-polarized N0 control neutrophils. The analysis was performed on the nCounter platform by NanoString using the PanCancer Immune Profiling Panel, which screens against 730 cancer-related genes.

Hierarchical clustering of pathway scores revealed that N1-and N2-like neutrophils take on distinct transcriptional profiles following *in vitro* polarization and that N2-like cells are more closely related to N0 control neutrophils **(Figure 4.10)**. In fact, the N1- and N2-polarized cells displayed opposite expression profiles for each pathway score. Interestingly, N1-like neutrophils upregulated their expression of genes associated with T-cell functions, cytotoxicity, adhesion and the TNF superfamily, whereas N2-polarized cells upregulated their expression of genes related to TLR and leukocyte functions.

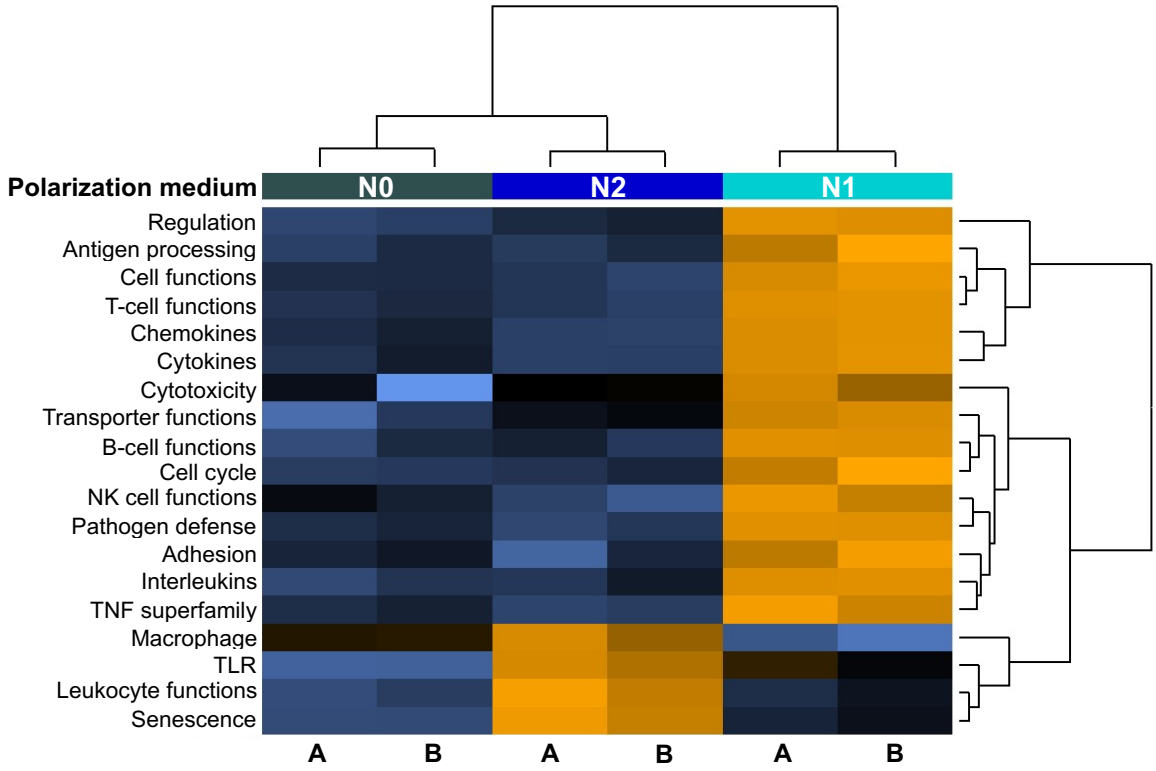

Figure 4.10. nCounter pathway analysis display opposite trends for N1-like and N2-like neutrophils. Primary human neutrophils isolated from two healthy blood donors were subjected to *in vitro* polarization based on a protocol by Mareike Ohms et al. (Ohms et al., 2020). N1- and N2-like cells were cultured in the presence of an N1- or N2 polarization cocktail containing caspase inhibitor Q-VD-OPh, whereas N0 control cells were treated with Q-VD-OPh only. N1-like and N0 cells were incubated at 37°C in a humidified air atmosphere containing 5% CO_2, whereas N2-like cells were incubated in a humidified hypoxic chamber at 37°C with 2% O_2 and 5% CO_2. RNA was isolated from neutrophils at 48h and analyzed on the nCounter platform by NanoString using the PanCancer Immune Profiling Panel, which screens against 730 cancer-related genes. Heatmap shows pathway scores across samples. Donor A data is indicated by the letter A and Donor B by the letter B. Orange indicates high scores, and blue indicates low scores. Branches indicate hierarchical clustering. Scores are displayed on the same scale via a Z-transformation.

N1 TANs have been described to suppress tumor progression through mechanisms associated with T-cell activation and cytotoxicity against tumor cells **(Figure 1.2)**. The finding that N1-like neutrophils upregulated pathways related to T-cell functions and adhesion could suggest that these cells, in likeness with the N1 TANs found *in vivo*, may be stimulatory for T-cells. In addition, the upregulation of genes associated with cytotoxicity and the TNF superfamily could link these cells to mechanisms involving cytotoxicity against tumor cells. The observation that N2-like TANs upregulated pathways associated with TLR- and leukocyte functions could suggest a role for these cells in promoting tumor progression through inflammatory signaling.

Plots displaying the most significantly differentially expressed genes emphasized the opposing effects of N1- and N2-polarization further. N1-like neutrophils upregulated genes associated with antigen presentation including sialic acid binding Ig-like lectin 1 (siglec-1), CD74, human leukocyte antigen-DR (HLA-DR) and transporter 2 (TAP-2), which could imply a capability for triggering T-cell responses (Lin et al., 2021, Beswick and Reyes, 2009, Wosen et al., 2018, Agrawal et al., 2004, Singhal et al., 2016) **(Figure 4.11A)**. In addition, several proinflammatory genes such as CXCL10, interferon induced protein 35 (IFI35), nuclear factor kappa-light chain enhancer of activated B-cells (NF-κB) and S100 calcium-binding protein A12 (S100A12) were upregulated by these cells (Ichikawa et al., 2013, Gounder et al., 2018, Liu et al., 2017, Foell et al., 2003).

N2-like neutrophils displayed upregulation of genes involved in neutrophil recruitment and migration including CXCR1, CD44, S100A12 and S100A8 (Lazennec and Richmond, 2010, Khan et al., 2004, Tardif et al., 2015) **(Figure 4.11B)**. In addition, the inflammatory cytokine macrophage migration inhibitory factor (MIF), which can prime neutrophils to undergo oxidative burst and NETosis, was highly upregulated (Schindler et al., 2021). Combined, the results of differential gene expression analysis revealed that N1- and N2-like neutrophils possess distinct expressional profiles. N1-like neutrophils upregulated genes involved in T-cell functions and cytotoxicity against T-cells, whereas N2-like neutrophils upregulated genes encoding proinflammatory mediators and migration-related factors.

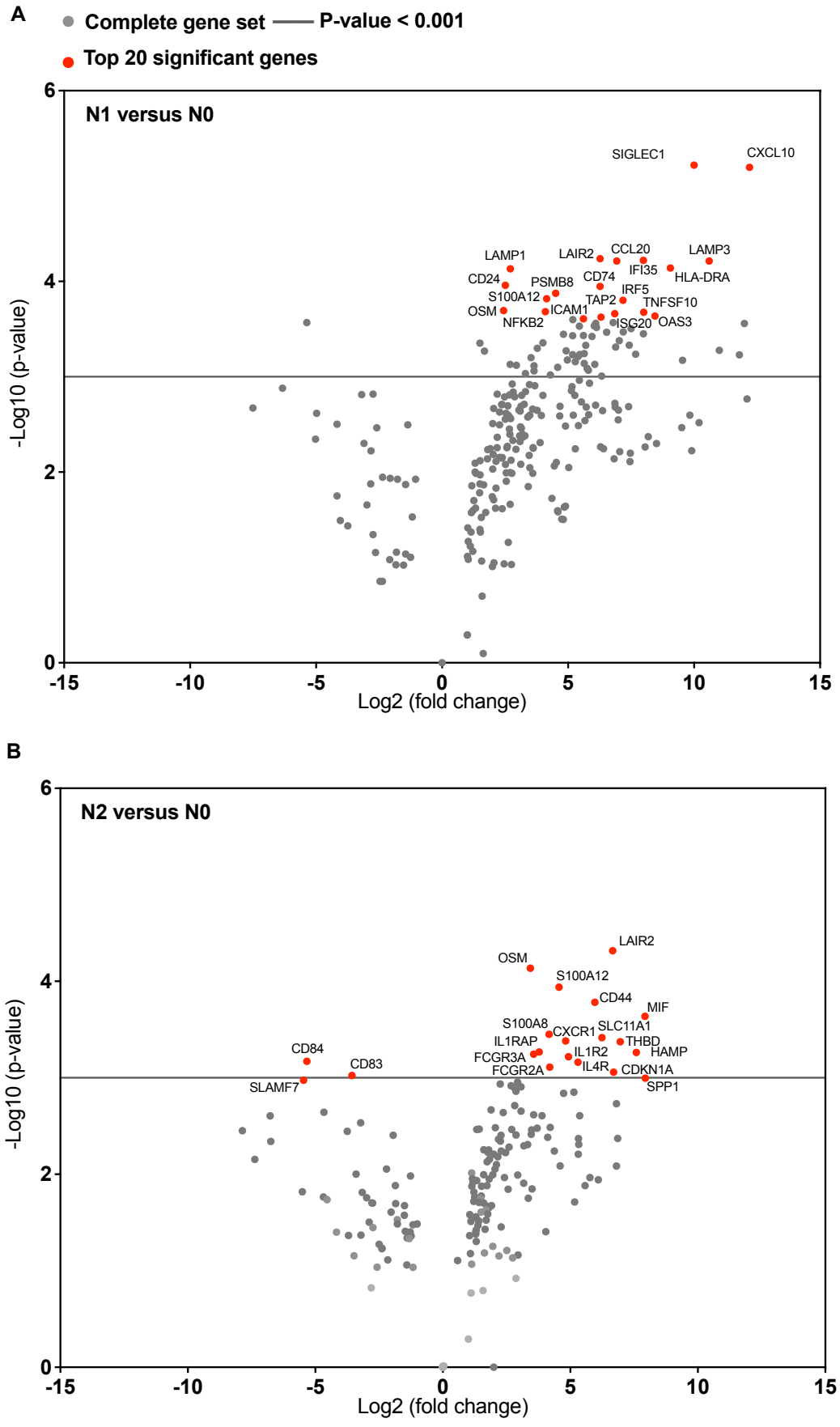
A
Complete gene set
P-value < 0.001
Top 20 significant genes
N1 versus N0
SIGLEC1
CXCL10
LAMP1
LAIR2
CCL20
LAMP3
IFI35
CD24
PSMB8
CD74
HLA-DRA
IRF5
S100A12
TAP2
TNFSF10
OSM
ICAM1
NFKB2
ISG20
OAS3
-Log10 (p-value)
Log2 (fold change)
B
N2 versus N0
LAIR2
OSM
S100A12
CD44
MIF
S100A8
CXCR1
SLC11A1
IL1RAP
THBD
CD84
CD83
FCGR3A
IL1R2
HAMP
FCGR2A
IL4R
CDKN1A
SLAMF7
SPP1
-Log10 (p-value)
Log2 (fold change)

Figure 4.11. nCounter differential gene expression analysis reveals distinct transcriptional profiles of N1-like and N2-like neutrophils. Primary human neutrophils isolated from two healthy blood donors were subjected to *in vitro* polarization based on a protocol by Mareike Ohms et al. (Ohms et al., 2020). N1- and N2-like cells were cultured in the presence of an N1- or N2 polarization cocktail containing caspase inhibitor Q-VD-OPh, whereas N0 control cells were treated with Q-VD-OPh only. N1-like and N0 cells were incubated at 37°C in a humidified air atmosphere containing 5% CO_2, whereas N2-like cells were incubated in a humidified hypoxic chamber at 37°C with 2% O_2 and 5% CO_2. RNA was isolated from neutrophils at 48h and analyzed on the nCounter platform by NanoString using the PanCancer Immune Profiling Panel, which screens against 730 cancer-related genes. Volcano plots show each gene's -log10(p-value) and log2(fold change). Highly statistical genes fall at the top of the plot and highly differentially expressed genes fall to either side. Horizontal lines indicate a p-value threshold of p = 0.001. The 20 most statistically significant genes are labeled in red.

4.3. TLR3-activation in colon cancer cells shifts *in vitro* polarization towards an N1-like phenotype

Neutrophils are enriched in several tumors, including those derived from colon cancer patients (Galdiero et al., 2016) (Unpublished data, Bugge et al., 2020), and have the ability to become polarized in their activities in response to the inflammatory signals present in the TME. Inflammation is initiated when immune receptors on cells in the TME recognize harmful stimuli and can contribute to suppression of tumorigenesis by activating an antitumorigenic immune response or promote malignant progression by fueling protumor functions. The best studied innate immune receptors are the TLRs, which are expressed on both immune cells and tumor cells.

In colon cancer cells, surface activation of TLR3 by the dsRNA analog poly(I:C) induces several neutrophil-attracting chemokines, including CXCL1-2, CXCL5-6, CXCL8 and CXCL10 (Bugge et al., 2017) (Unpublished data, Bugge et al., 2020). In addition, supernatant from such TLR3-activated cells has been demonstrated to attract neutrophils *in vitro* (Unpublished data, Bugge et al., 2020), which suggest that these cells may also be capable of neutrophil polarization. In order to investigate whether TLR3-activation in colon cancer cells induce secretion of factors that can polarize neutrophils, SW620 cells were stimulated with poly(I:C) for 24h before supernatant was collected and added to primary human neutrophils. The supernatant-treated neutrophils were assayed for their expression of selected surface markers by staining with fluorescently conjugated antibodies and flow cytometry. These cells were then compared to N0 control, N1-like and N2-like cells cultured in parallel to determine if neutrophil polarization was shifted in one or the other direction.

4.3.1. Purity assessment of freshly isolated neutrophils

Neutrophils were isolated from two healthy blood donors and assessed for purity against T-cells and monocytes as described in **Section 4.1.2**. FSC-A and SSC-A, and gating strategy is shown in **Figure**

4.12A. Staining against granulocyte CD15 and CD66b displayed seemingly pure neutrophil populations for both donors (indicated by green gates) **(Figure 4.12B)**. Less than 1% of cells stained positively for contaminating CD3 T-cells (~0%) **(Figure 4.12C)** or CD14 monocytes (~0.2%) **(Figure 4.12D)**. These results indicate neutrophils of ~95-97% purity.

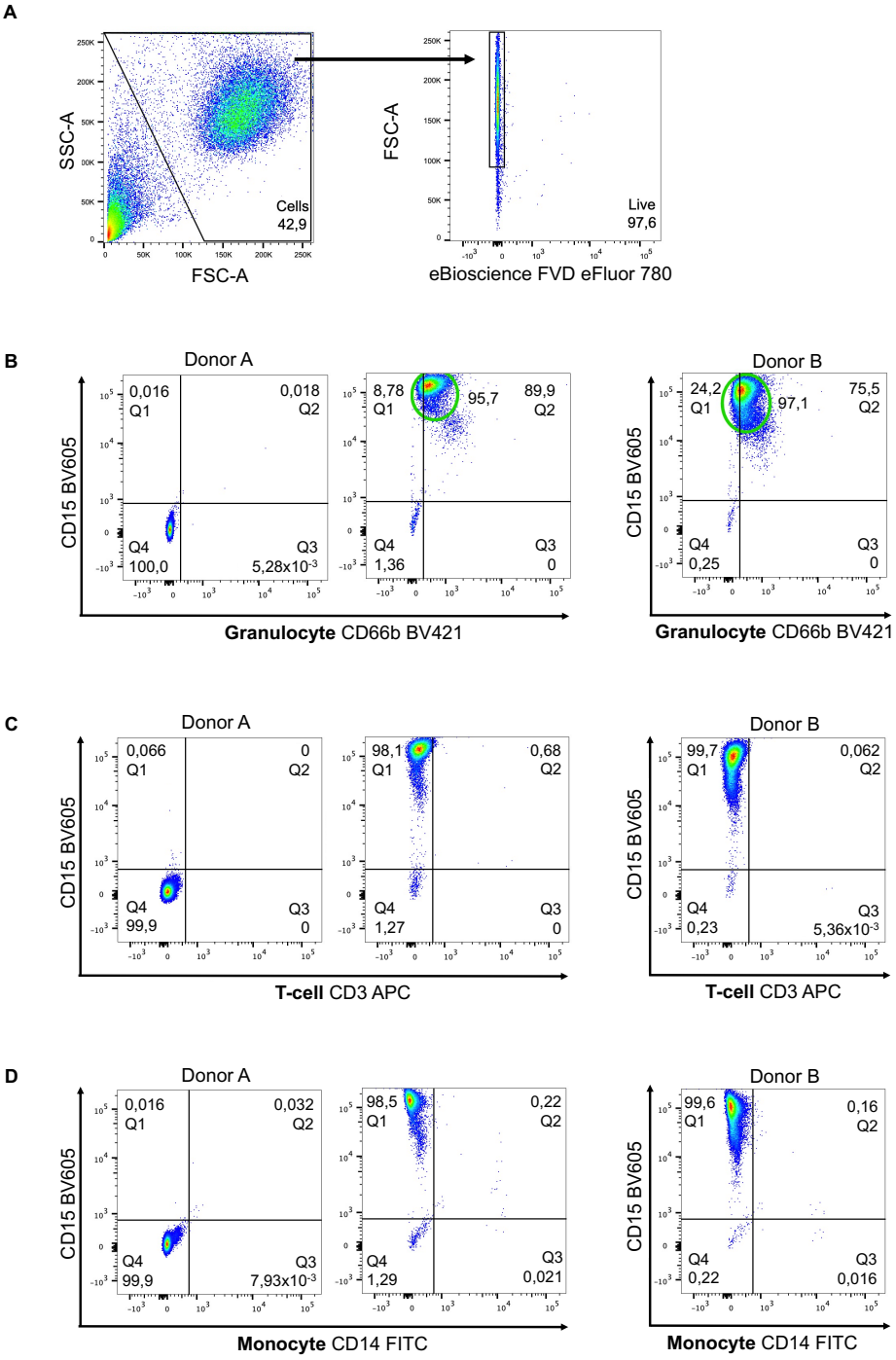

Figure 4.12. Purity assessment of isolated neutrophils. Primary human neutrophils isolated from two healthy blood donors were stained with antibodies and eBioscience FVD eFluor 780, and analyzed with compensation on a BD LSR II flow cytometer (BD). The data was gated to remove debris (FSC-A/SSC-A) and dead cells (eBioscience FVD eFluor 780/FSC-A) **(A)**. An unstained control from Donor A was used to set the quadrants and defined single positive cells (Q1 and Q3), double positive cells (Q2) and double negative cells (Q4). Bivariate plots show neutrophil purity assessed against granulocyte CD66b **(B)** T-cell CD3 **(C)** and monocyte CD14 **(D)**. Numbers in gates represent frequencies.

4.3.2. Supernatant from poly(I:C)-stimulated colon cancer cells activate primary human neutrophils

The freshly isolated neutrophils were incubated with supernatant collected from TLR3-activated SW620 cells at 37°C in a humidified air atmosphere containing 5% CO_2 for 48h. Neutrophils were also incubated with supernatants harvested from medium-stimulated cancer cells and from poly(I:C)/medium-stimulated knockdown cancer cells to verify that the release of polarizing factors was TLR3-specific. In addition, neutrophils were stimulated with poly(I:C) ligand to validate that the polarization occurred in response to SW620-derived factors and not in response to poly(I:C) present in the supernatants. The different treatments are illustrated in **Figure 4.13**. Since neutrophils are prone to spontaneous apoptosis, the experiments were performed in the presence of a caspase inhibitor.

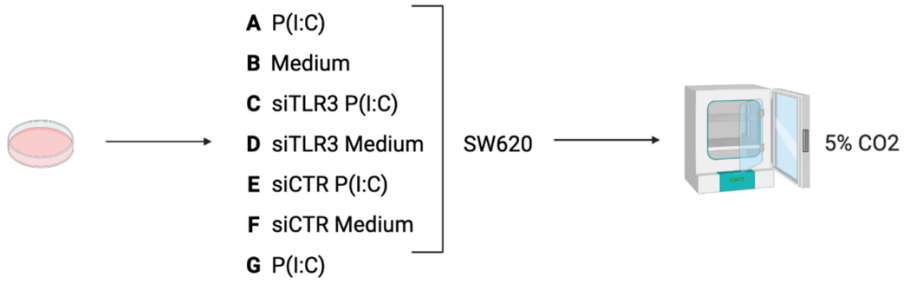

Figure 4.13. Experimental setup for testing the polarization potential of TLR3-activated colon cancer cells. Primary human neutrophils isolated from healthy blood donors were treated with supernatants (250 μL) collected from poly(I:C) (P(I:C)) or medium-stimulated SW620 cells **(A-B)** and TLR3- (siTLR3) **(C-D)** or control (siCTR) **(E-F)** knockdown SW620 cells. In addition, neutrophils were treated with P(I:C) ligand **(G)**. Neutrophils were incubated at 37°C in a humidified air atmosphere containing 5% CO_2 for 48h. Because neutrophils are prone to spontaneous apoptosis, the experiments were performed in the presence of the caspase inhibitor Q-VD-OPh (3μM). *Created with BioRender.com*

Supernatant-treated neutrophils from two donors were harvested at 48h and compared to N0, N1- and N2-like cells by antibody staining and flow cytometry. Upon treatment with supernatant collected from poly(I:C)-stimulated colon cancer cells, neutrophils displayed decreased expression of the N2-marker CXCR2, similar to N1-polarized neutrophils **(Figure 4.14A and Figure 15A)**. The expression of the N1-marker CD95 was slightly upregulated compared to the N0 control and N2-like cells **(Figure 4.14B**

and Figure 4.15B), whereas the expression of CD54 was increased compared to these cells but not as high as that of the N1-like cells **(Figure 4.14C and Figure 4.15C)**.

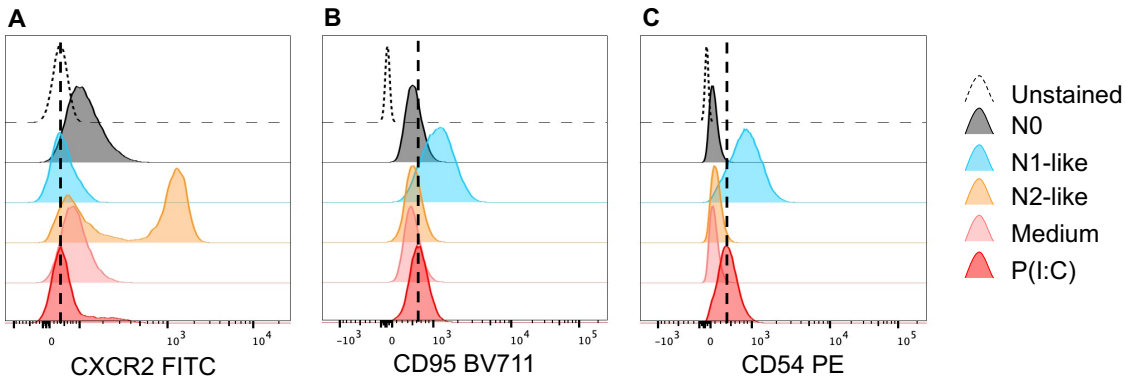

Figure 4.14. Histograms of CXCR2, CD95 and CD54 expression on supernatant-treated neutrophils. Primary human neutrophils isolated from two healthy blood donors were treated with supernatants collected from poly(I:C) (P(I:C)) or medium-stimulated SW620 colon cancer cells and TLR3 (siTLR3) or control (siCTR) knockdown cells. In addition, neutrophils were treated with P(I:C) ligand. Neutrophils were incubated at 37°C in a humidified air atmosphere containing 5% CO_2 for 48h. Because neutrophils are prone to spontaneous apoptosis, the experiments were performed in the presence of the caspase inhibitor Q-VD-OPh. N0 control, N1-like and N2-like neutrophils were grown in parallel based on a protocol by Mareike Ohms et al. (Ohms et al., 2020). Cells were assayed at 48h for their expression of surface CXCR2 **(A)**, CD95/Fas **(B)** and CD54/ICAM-1 **(C)** by staining with antibodies and flow cytometry. The analysis was performed with compensation on a BD LSR II flow cytometer (BD). Flow cytometry data was gated as described in **Figure 4.4**. Histograms show representative plots for donor B scaled to the mode.

The TLR3 knockdown controls displayed similar expression of CXCR2 **(Figure 4.15A)** and CD95 **(Figure 4.15B)** to N0 neutrophils, but the siTLR3 poly(I:C) cells upregulated their expression of CD54 **(Figure 4.15C)**. The poly(I:C) ligand control expressed similar levels of these markers to the N0 control, suggesting that polarization was due to factors released from the SW620 cells upon poly(I:C)-stimulation. The poly(I:C) ligand control expressed similar levels of these markers to the N0 control, suggesting that polarization was due to factors released from the SW620 cells upon poly(I:C)-stimulation. The expression of the activation markers CD62L, CD11b and CD66b on neutrophils treated with supernatant collected from poly(I:C)-stimulated colon cancer cells was more similar to N1-like neutrophils than N2-like neutrophils. Compared to the siTLR3 P(I:C) control, these cells displayed similar shedding of CD62L **(Figure 4.15D)** but upregulated their expression of CD11b **(Figure 4.15E)** and CD66b **(Figure 4.15F)**. The poly(I:C) ligand control showed similar levels of each marker to N0 neutrophils. Combined these results suggest that TLR3-activation in colon cancer cells might induce polarization towards an N1-direction.

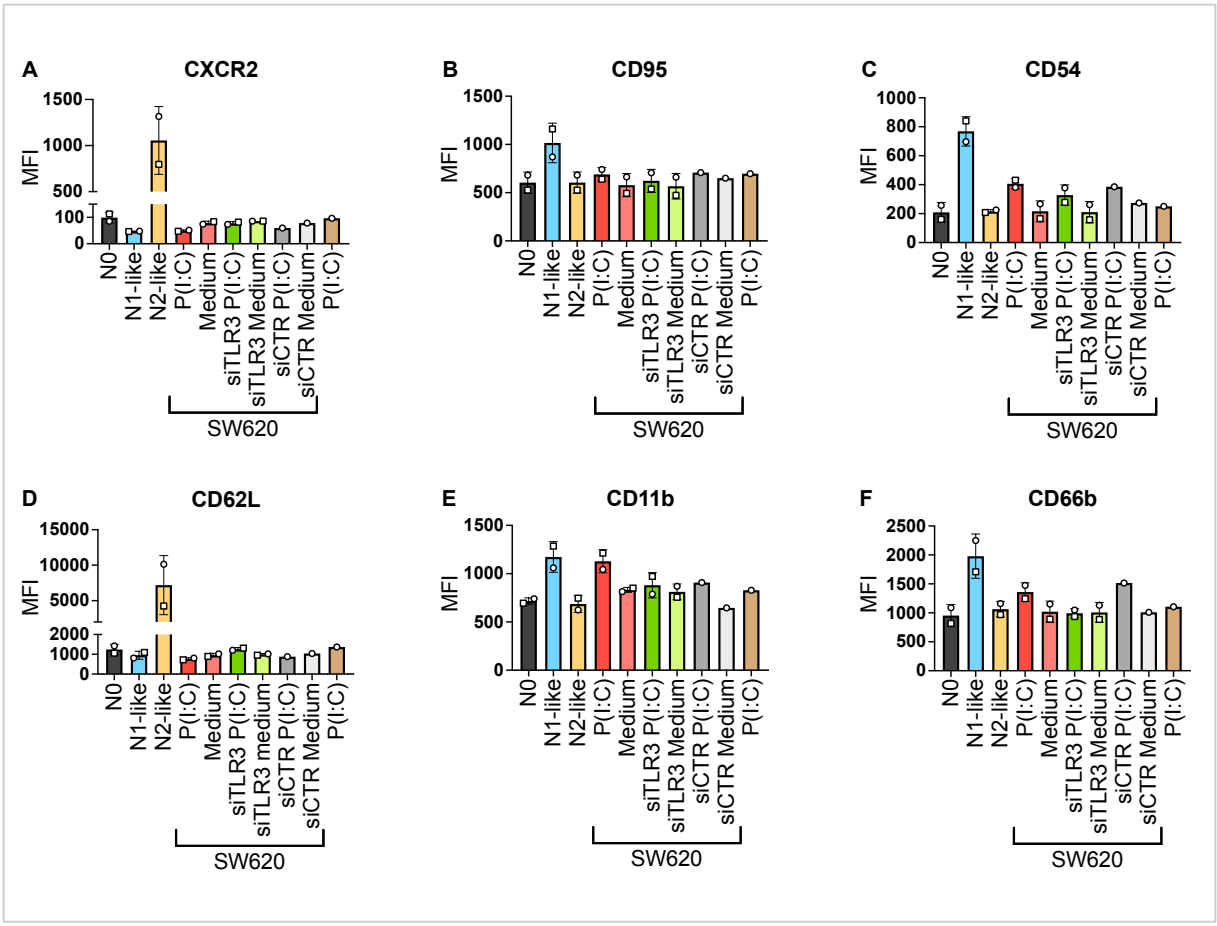

Figure 4.15. Expression of polarization- and activation markers on supernatant-treated neutrophils. Primary human neutrophils isolated from two healthy blood donors were treated with supernatants collected from poly(I:C) (P(I:C)) or medium-stimulated SW620 colon cancer cells and TLR3 (siTLR3) or control (siCTR) knockdown cells. In addition, neutrophils were treated with P(I:C) ligand. Neutrophils were incubated at 37°C in a humidified air atmosphere containing 5% CO_2 for 48h. Because neutrophils are prone to spontaneous apoptosis, the experiments were performed in the presence of the caspase inhibitor Q-VD-OPh (3μM). N0 control, N1-like and N2-like neutrophils were grown in parallel based on a protocol by Mareike Ohms et al. (Ohms et al., 2020). Cells were assayed at 48h for their expression of surface CXCR2 **(A)**, CD95/Fas **(B)**, CD54/ICAM-1 **(C)**, CD62L/L-selectin **(D)**, CD11b/integrin alpha M **(E)** and CD66b/CEACAM8 **(F)** by staining with antibodies and flow cytometry. The analysis was performed with compensation on a BD LSR II flow cytometer (BD). Bar plots show median fluorescence intensity (MFI) ± SD (n=2) with donor A data presented as circles and Donor B data indicated by squares. Flow cytometry data was gated as described in **Figure 4.4**.

4.3.3. Viability of neutrophils after 24- and 48h polarization

The percentage of viable cells at 48h was determined as described in section **Section 4.1.4** and is summarized in **Figure 4.16**. These results suggest that factors released from poly(I:C)-stimulated colon cancer cells do not affect cell viability when compared to the N0 control.

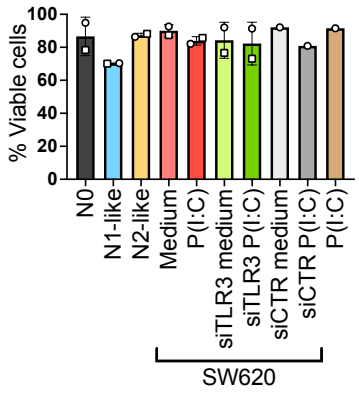

Figure 4.16. Percentage of viable cells at 48h. Primary human neutrophils isolated from two healthy blood donors were treated with supernatants collected from poly(I:C) (P(I:C)) or medium-stimulated SW620 colon cancer cells and TLR3 (siTLR3) or control (siCTR) knockdown cells. In addition, neutrophils were treated with P(I:C) ligand. Neutrophils were incubated at 37°C in a humidified air atmosphere containing 5% CO_2 for 48h. Because neutrophils are prone to spontaneous apoptosis, the experiments were performed in the presence of the caspase inhibitor Q-VD-OPh (3μM). N0 control, N1-like and N2-like neutrophils were grown in parallel based on a protocol by Mareike Ohms et al. (Ohms et al., 2020). Cells were harvested at 48h, stained with Annexin $A5^{FITC}$ and eBioscience FVD eFluor 780 before analyzed with compensation on a BD LSR II flow cytometer (BD). The data was gated as described in **Figure 4.8**. Bar plots show viability at 48h $\pm$ SD (n=2). Donor A data are presented as circles and Donor B data are indicated by squares.

5. Discussion

Neutrophils have traditionally been considered as homogenous cells whose main function is to fight infections. However, accumulating evidence has revealed that these abundant leukocytes present a larger heterogeneity than first presumed. The observation that neutrophils take on different phenotypes under healthy and pathological conditions has sparked a renewed interest in neutrophil biology. This is particularly true in the setting of cancer, in which the important role of neutrophils is emphasized by their accumulation in circulation and the TME, and their dual role in tumorigenesis.

Thus far, most studies investigating the dual role of neutrophils in cancer have involved murine tumor models. However, human and murine neutrophils display several differences and the neutrophil responses observed in murine tumor systems may not translate to humans, thus leaving a major knowledge gap. For instance, neutrophils constitute as much as 50-70% of circulating leukocytes in humans but are less common in mice, where they only account for 10-30% (Eruslanov et al., 2017). In addition, many chemokines and receptors that influence neutrophil migration in humans are absent in mice and the activation pathway of ROS production differ between human and mouse neutrophils (Eruslanov et al., 2017).

The method for *in vitro* polarization reported by Ohms et al. (Ohms et al., 2020) appears to provide a system that has potential to assist in closing the knowledge gap between murine and human neutrophils in cancer. The results of this preliminary study aligned nicely with the findings reported by Ohms et al. and the N1-like and N2-like neutrophils were revealed to exhibit similar relative levels of N1 and N2 surface markers to what was reported in the Ohms et al. protocol. In accordance with their findings, the N1-like neutrophils were characterized as $CD95^{high}$ $CD54^{high}$ $CXCR2^{low}$, whereas N2-like cells were $CXCR2^{high}$ $CD95^{low}$ $CD54^{low}$ **(Figure 4.5)**. In addition, the data indicated an activated state of N1-like neutrophils compared to N2-like neutrophils **(Figure 4.6)**. Similar production of inflammatory mediators was also observed, with the exception of the chemoattractant CXCL8, which contrary to the findings by Ohms et al. was observed to be highest for N1-like and not N2-like neutrophils **(Figure 4.7)**.

Further characterization of these N1-like and N2-like cells by nCounter gene expression analysis revealed opposing trends in pathway regulation **(Figure 4.10)**. N1-like neutrophils were shown to upregulate pathways associated with T-cell functions, cytotoxicity, adhesion and the TNF superfamily, which links these cells to N1 antitumor mechanisms such as T-cell stimulation and cytotoxicity against tumor cells. N2-like neutrophils upregulated pathways related to TLR and leukocyte functions, suggesting that these cells can induce protumor N2 mechanisms through inflammatory signaling. Still, because purity assessment **(Figure 4.2)** revealed 5-10% contamination with cells of unclear nature, care must be taken when interpreting these preliminary results and the experiment should be repeated to verify the significance of these findings.

Importantly, the preliminary results from this study also suggested that this *in vitro* polarization model can be employed to investigate how inflammatory signaling in cancer cells influence the polarization of human neutrophils. Thus, the model also provides a system for the elucidation of the molecular mechanisms inducing anti- and pro-tumorigenic neutrophils in different types of cancer. Neutrophils are double-edged swords in cancer development and targeting strategies should be developed to not only disrupt pro-tumorigenic behaviors, but also retain the anti-tumor potential of neutrophils. Further research of the exact roles, recruitment pathways and molecular mechanisms of TANs is essential to develop therapeutic approaches with maximal level of therapeutic benefits and minimal risk of dangerous side effects.

6. Conclusion

This study evaluated and verified a newly reported model for *in vitro* polarization of human neutrophils. In addition, preliminary findings revealed that the generated N1-like and N2-like neutrophils displayed distinct transcriptional profiles. Finally, the study also demonstrated the use for the *in vitro* polarization model in the investigation of how signaling from cancer cells affect human neutrophils. Future research should focus on investigating the characteristics of these N1-like and N2-like subsets further, in terms of surface markers, expressional markers and effector functions.

Supplementary

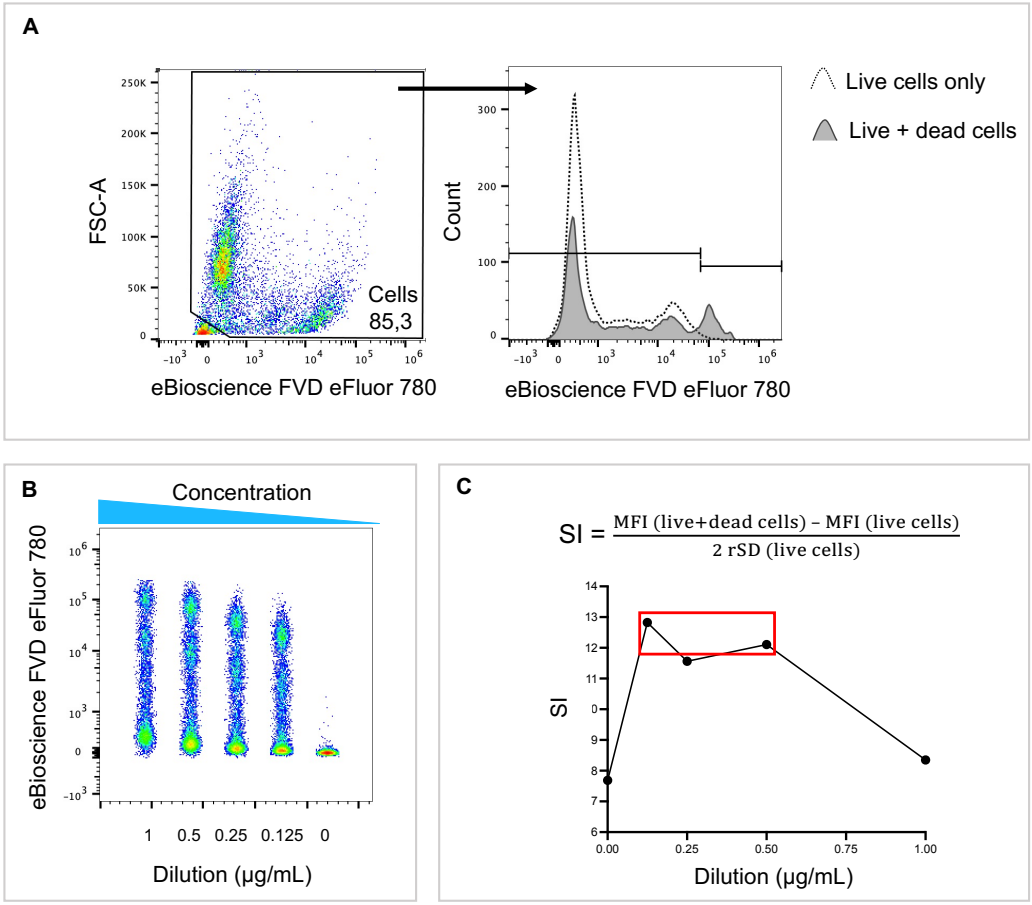

Supplementary Figure 1. The optimal staining concentration for viability dye is 0.5 μg/mL. Samples containing live and live and dead THP-1 cells were stained with 1-, 0.5-, 0.25-, 0.125 and 0 μg/mL of eBioscience FVD eFluor 780 and analyzed on a BD LSR II flow cytometer (BD). The data was gated to remove debris before populations that were negative (live cells) and positive (dead cells) for the dye were defined **(A)**. The spread of live and dead cell populations for each staining concentration is displayed in **B**. The staining index (SI) for each concentration was calculated as described in **C**. The red square indicates appropriate SI.

References

ADAN, A., ALIZADA, G., KIRAZ, Y., BARAN, Y. & NALBANT, A. 2017. Flow cytometry: basic principles and applications. *Crit Rev Biotechnol,* 37**,** 163-176.

AGRAWAL, S., REEMTSMA, K., BAGIELLA, E., OLUWOLE, S. F. & BRAUNSTEIN, N. S. 2004. Role of TAP-1 and/or TAP-2 antigen presentation defects in tumorigenicity of mouse melanoma. *Cell Immunol,* 228**,** 130-7.

AI, L., MU, S., WANG, Y., WANG, H., CAI, L., LI, W. & HU, Y. 2018. Prognostic role of myeloid-derived suppressor cells in cancers: a systematic review and meta-analysis. *BMC Cancer,* 18**,** 1220.

ALLENDORF, D. J., YAN, J., ROSS, G. D., HANSEN, R. D., BARAN, J. T., SUBBARAO, K., WANG, L. & HARIBABU, B. 2005. C5a-mediated leukotriene B4-amplified neutrophil chemotaxis is essential in tumor immunotherapy facilitated by anti-tumor monoclonal antibody and beta-glucan. *J Immunol,* 174**,** 7050-6.

ANDERSON, N. M. & SIMON, M. C. 2020. The tumor microenvironment. *Curr Biol,* 30**,** R921-R925.

ANDZINSKI, L., KASNITZ, N., STAHNKE, S., WU, C. F., GEREKE, M., VON KOCKRITZ-BLICKWEDE, M., SCHILLING, B., BRANDAU, S., WEISS, S. & JABLONSKA, J. 2016. Type I IFNs induce anti-tumor polarization of tumor associated neutrophils in mice and human. *Int J Cancer,* 138**,** 1982-93.

ATRI, C., GUERFALI, F. Z. & LAOUINI, D. 2018. Role of Human Macrophage Polarization in Inflammation during Infectious Diseases. *International Journal of Molecular Sciences,* 19.

AYDIN, S. 2015. A short history, principles, and types of ELISA, and our laboratory experience with peptide/protein analyses using ELISA. *Peptides,* 72**,** 4-15.

BERRY, R. S., XIONG, M. J., GREENBAUM, A., MORTAJI, P., NOFCHISSEY, R. A., SCHULTZ, F., MARTINEZ, C., LUO, L., MORRIS, K. T. & HANSON, J. A. 2017. High levels of tumor-associated neutrophils are associated with improved overall survival in patients with stage II colorectal cancer. *PLoS One,* 12**,** e0188799.

BESWICK, E. J. & REYES, V. E. 2009. CD74 in antigen presentation, inflammation, and cancers of the gastrointestinal tract. *World J Gastroenterol,* 15**,** 2855-61.

BOCHNER, B. S., STERBINSKY, S. A., BICKEL, C. A., WERFEL, S., WEIN, M. & NEWMAN, W. 1994. Differences between Human Eosinophils and Neutrophils in the Function and Expression of Sialic Acid-Containing Counterligands for E-Selectin. *Journal of Immunology,* 152**,** 774-782.

BUGGE, M., BERGSTROM, B., EIDE, O. K., SOLLI, H., KJONSTAD, I. F., STENVIK, J., ESPEVIK, T. & NILSEN, N. J. 2017. Surface Toll-like receptor 3 expression in metastatic intestinal epithelial cells induces inflammatory cytokine production and promotes invasiveness. *J Biol Chem,* 292**,** 15408-15425.

CASBON, A. J., REYNAUD, D., PARK, C., KHUC, E., GAN, D. D., SCHEPERS, K., PASSEGUE, E. & WERB, Z. 2015. Invasive breast cancer reprograms early myeloid differentiation in the bone marrow to generate immunosuppressive neutrophils. *Proc Natl Acad Sci U S A,* 112**,** E566-75.

CHAKRABORTY, A. & GUHA, S. 2007. Granulocyte colony-stimulating factor/granulocyte colony-stimulating factor receptor biological axis promotes survival and growth of bladder cancer cells. *Urology,* 69**,** 1210-5.

CHAO, T., FURTH, E. E. & VONDERHEIDE, R. H. 2016. CXCR2-Dependent Accumulation of Tumor-Associated Neutrophils Regulates T-cell Immunity in Pancreatic Ductal Adenocarcinoma. *Cancer Immunol Res,* 4**,** 968-982.

COFFELT, S. B., WELLENSTEIN, M. D. & DE VISSER, K. E. 2016. Neutrophils in cancer: neutral no more. *Nature Reviews Cancer,* 16**,** 431-446.

COWLAND, J. B. & BORREGAARD, N. 2016. Granulopoiesis and granules of human neutrophils. *Immunological Reviews,* 273**,** 11-28.

DAJON, M., IRIBARREN, K. & CREMER, I. 2017. Toll-like receptor stimulation in cancer: A pro- and anti-tumor double-edged sword. *Immunobiology,* 222**,** 89-100.

DALE, D. C. 2009. Advances in the treatment of neutropenia. *Curr Opin Support Palliat Care,* 3**,** 207-12.

DANCEY, J. T., DEUBELBEISS, K. A., HARKER, L. A. & FINCH, C. A. 1976. Neutrophil kinetics in man. *J Clin Invest,* 58**,** 705-15.

DERYUGINA, E. I. & QUIGLEY, J. P. 2006. Matrix metalloproteinases and tumor metastasis. *Cancer and Metastasis Reviews,* 25**,** 9-34.

DUCKER, T. P. & SKUBITZ, K. M. 1992. Subcellular localization of CD66, CD67, and NCA in human neutrophils. *J Leukoc Biol,* 52**,** 11-6.

EBRAHEM, Q., CHAURASIA, S. S., VASANJI, A., QI, J. H., KLENOTIC, P. A., CUTLER, A., ASOSINGH, K., ERZURUM, S. & ANAND-APTE, B. 2010. Cross-talk between vascular endothelial growth factor and matrix metalloproteinases in the induction of neovascularization in vivo. *Am J Pathol,* 176**,** 496-503.

ELLIS, T. N. & BEAMAN, B. L. 2004. Interferon-gamma activation of polymorphonuclear neutrophil function. *Immunology,* 112**,** 2-12.

ERMERT, D., ZYCHLINSKY, A. & URBAN, C. 2009. Fungal and bacterial killing by neutrophils. *Methods Mol Biol,* 470**,** 293-312.

ERUSLANOV, E. B., BHOJNAGARWALA, P. S., QUATROMONI, J. G., STEPHEN, T. L., RANGANATHAN, A., DESHPANDE, C., AKIMOVA, T., VACHANI, A., LITZKY, L., HANCOCK, W. W., CONEJO-GARCIA, J. R., FELDMAN, M., ALBEIDA, S. M. & SINGHAL, S. 2014. Tumor-associated neutrophils stimulate T cell responses in early-stage human lung cancer. *Journal of Clinical Investigation,* 124**,** 5466-5480.

ERUSLANOV, E. B., SINGHAL, S. & ALBELDA, S. M. 2017. Mouse versus Human Neutrophils in Cancer: A Major Knowledge Gap. *Trends Cancer,* 3**,** 149-160.

FOELL, D., KUCHARZIK, T., KRAFT, M., VOGL, T., SORG, C., DOMSCHKE, W. & ROTH, J. 2003. Neutrophil derived human S100A12 (EN-RAGE) is strongly expressed during chronic active inflammatory bowel disease. *Gut,* 52**,** 847-53.

FRIDLENDER, Z. G. & ALBELDA, S. M. 2012. Tumor-associated neutrophils: friend or foe? *Carcinogenesis,* 33**,** 949-55.

FRIDLENDER, Z. G., SUN, J., KIM, S., KAPOOR, V., CHENG, G., LING, L., WORTHEN, G. S. & ALBELDA, S. M. 2009. Polarization of tumor-associated neutrophil phenotype by TGF-beta: "N1" versus "N2" TAN. *Cancer Cell,* 16**,** 183-94.

FRIDLENDER, Z. G., SUN, J., MISHALIAN, I., SINGHAL, S., CHENG, G., KAPOOR, V., HORNG, W., FRIDLENDER, G., BAYUH, R., WORTHEN, G. S. & ALBELDA, S. M. 2012. Transcriptomic analysis comparing tumor-associated neutrophils with granulocytic myeloid-derived suppressor cells and normal neutrophils. *PLoS One,* 7**,** e31524.

GALDIERO, M. R., BIANCHI, P., GRIZZI, F., DI CARO, G., BASSO, G., PONZETTA, A., BONAVITA, E., BARBAGALLO, M., TARTARI, S., POLENTARUTTI, N., MALESCI, A., MARONE, G., RONCALLI, M., LAGHI, L., GARLANDA, C., MANTOVANI, A. & JAILLON, S. 2016. Occurrence and significance of tumor-associated neutrophils in patients with colorectal cancer. *Int J Cancer,* 139**,** 446-56.

GERLINI, G., TUN-KYI, A., DUDLI, C., BURG, G., PIMPINELLI, N. & NESTLE, F. O. 2004. Metastatic melanoma secreted IL-10 down-regulates CD1 molecules on dendritic cells in metastatic tumor lesions. *Am J Pathol,* 165**,** 1853-63.

GOMES, N. E., BRUNIALTI, M. K., MENDES, M. E., FREUDENBERG, M., GALANOS, C. & SALOMAO, R. 2010. Lipopolysaccharide-induced expression of cell surface receptors and cell activation of neutrophils and monocytes in whole human blood. *Braz J Med Biol Res,* 43**,** 853-8.

GOPINATH, R. & NUTMAN, T. B. 1997. Identification of eosinophils in lysed whole blood using side scatter and CD16 negativity. *Cytometry,* 30**,** 313-316.

GOUNDER, A. P., YOKOYAMA, C. C., JARJOUR, N. N., BRICKER, T. L., EDELSON, B. T. & BOON, A. C. M. 2018. Interferon induced protein 35 exacerbates H5N1 influenza disease through the expression of IL-12p40 homodimer. *PLoS Pathog,* 14**,** e1007001.

GRANOT, Z., HENKE, E., COMEN, E. A., KING, T. A., NORTON, L. & BENEZRA, R. 2011. Tumor entrained neutrophils inhibit seeding in the premetastatic lung. *Cancer Cell,* 20**,** 300-14.

GREENHOUGH, A., SMARTT, H. J., MOORE, A. E., ROBERTS, H. R., WILLIAMS, A. C., PARASKEVA, C. & KAIDI, A. 2009. The COX-2/PGE2 pathway: key roles in the hallmarks of cancer and adaptation to the tumour microenvironment. *Carcinogenesis,* 30**,** 377-86.

GUTHRIE, G. J., CHARLES, K. A., ROXBURGH, C. S., HORGAN, P. G., MCMILLAN, D. C. & CLARKE, S. J. 2013. The systemic inflammation-based neutrophil-lymphocyte ratio: experience in patients with cancer. *Crit Rev Oncol Hematol,* 88**,** 218-30.

HANAHAN, D. & WEINBERG, R. A. 2011. Hallmarks of Cancer: The Next Generation. *Cell,* 144**,** 646-674.

HANNON, G. J. 2002. RNA interference. *Nature,* 418**,** 244-51.

HOUGHTON, A. M., RZYMKIEWICZ, D. M., JI, H. B., GREGORY, A. D., EGEA, E. E., METZ, H. E., STOLZ, D. B., LAND, S. R., MARCONCINI, L. A., KLIMENT, C. R., JENKINS, K. M., BEAULIEU, K. A., MOUDED, M., FRANK, S. J., WONG, K. K. & SHAPIRO, S. D. 2010. Neutrophil elastase-mediated degradation of IRS-1 accelerates lung tumor growth. *Nature Medicine,* 16**,** 219-U127.

ICHIKAWA, A., KUBA, K., MORITA, M., CHIDA, S., TEZUKA, H., HARA, H., SASAKI, T., OHTEKI, T., RANIERI, V. M., DOS SANTOS, C. C., KAWAOKA, Y., AKIRA, S., LUSTER, A. D., LU, B., PENNINGER, J. M., UHLIG, S., SLUTSKY, A. S. & IMAI, Y. 2013. CXCL10-CXCR3 enhances the development of neutrophil-mediated fulminant lung injury of viral and nonviral origin. *Am J Respir Crit Care Med,* 187**,** 65-77.

IVETIC, A. 2018. A head-to-tail view of L-selectin and its impact on neutrophil behaviour. *Cell Tissue Res,* 371**,** 437-453.

JABLONSKA, J., LESCHNER, S., WESTPHAL, K., LIENENKLAUS, S. & WEISS, S. 2010. Neutrophils responsive to endogenous IFN-beta regulate tumor angiogenesis and growth in a mouse tumor model. *J Clin Invest,* 120**,** 1151-64.

JOHANSSON, M., DENARDO, D. G. & COUSSENS, L. M. 2008. Polarized immune responses differentially regulate cancer development. *Immunol Rev,* 222**,** 145-54.

JOYCE, J. A. 2005. Therapeutic targeting of the tumor microenvironment. *Cancer Cell,* 7**,** 513-20.

KHAN, A. I., KERFOOT, S. M., HEIT, B., LIU, L., ANDONEGUI, G., RUFFELL, B., JOHNSON, P. & KUBES, P. 2004. Role of CD44 and hyaluronan in neutrophil recruitment. *J Immunol,* 173**,** 7594-601.

KOLACZKOWSKA, E. & KUBES, P. 2013. Neutrophil recruitment and function in health and inflammation. *Nat Rev Immunol,* 13**,** 159-75.

Kreftregisteret, "Nøkkeltall om kreft" [online], https://www.kreftregisteret.no/Temasider/om-kreft/ (accessed 18 May 2021).

LAMBERT, C., PREIJERS, F., YANIKKAYA DEMIREL, G. & SACK, U. 2017. Monocytes and macrophages in flow: an ESCCA initiative on advanced analyses of monocyte lineage using flow cytometry. *Cytometry B Clin Cytom,* 92**,** 180-188.

LAZENNEC, G. & RICHMOND, A. 2010. Chemokines and chemokine receptors: new insights into cancer-related inflammation. *Trends Mol Med,* 16**,** 133-44.

LECOT, P., SARABI, M., PEREIRA ABRANTES, M., MUSSARD, J., KOENDERMAN, L., CAUX, C., BENDRISS-VERMARE, N. & MICHALLET, M. C. 2019. Neutrophil Heterogeneity in Cancer: From Biology to Therapies. *Front Immunol,* 10**,** 2155.

LEONE, R. D. & EMENS, L. A. 2018. Targeting adenosine for cancer immunotherapy. *J Immunother Cancer,* 6**,** 57.

LI, Z., ZHAO, R., CUI, Y., ZHOU, Y. & WU, X. 2018. The dynamic change of neutrophil to lymphocyte ratio can predict clinical outcome in stage I-III colon cancer. *Sci Rep,* 8**,** 9453.

LIEW, P. X. & KUBES, P. 2019. The Neutrophil's Role During Health and Disease. *Physiol Rev,* 99**,** 1223-1248.

LIN, C. H., YEH, Y. C. & YANG, K. D. 2021. Functions and therapeutic targets of Siglec-mediated infections, inflammations and cancers. *J Formos Med Assoc,* 120**,** 5-24.

LIU, I. L., TSAI, C. H., HSU, C. H., HU, J. M., CHEN, Y. C., TIAN, Y. F., YOU, S. L., CHEN, C. Y., HSIAO, C. W., LIN, C. Y., CHOU, Y. C. & SUN, C. A. 2019. Helicobacter pylori infection and the risk of colorectal cancer: a nationwide population-based cohort study. *QJM,* 112**,** 787-792.

LIU, T., ZHANG, L., JOO, D. & SUN, S. C. 2017. NF-kappaB signaling in inflammation. *Signal Transduct Target Ther,* 2.

MANFROI, B., MOREAUX, J., RIGHINI, C., GHIRINGHELLI, F., STURM, N. & HUARD, B. 2018. Tumor-associated neutrophils correlate with poor prognosis in diffuse large B-cell lymphoma patients. *Blood Cancer J,* 8**,** 66.

MATLUNG, H. L., BABES, L., ZHAO, X. W., VAN HOUDT, M., TREFFERS, L. W., VAN REES, D. J., FRANKE, K., SCHORNAGEL, K., VERKUIJLEN, P., JANSSEN, H., HALONEN, P., LIEFTINK, C., BEIJERSBERGEN, R. L., LEUSEN, J. H. W., BOELENS, J. J., KUHNLE, I., VAN DER WERFF TEN BOSCH, J., SEEGER, K., RUTELLA, S., PAGLIARA, D., MATOZAKI, T., SUZUKI, E., MENKE-VAN DER HOUVEN VAN OORDT, C. W., VAN BRUGGEN, R., ROOS, D., VAN LIER, R. A. W., KUIJPERS, T. W., KUBES, P. & VAN DEN BERG, T. K. 2018. Neutrophils Kill Antibody-Opsonized Cancer Cells by Trogoptosis. *Cell Rep,* 23**,** 3946-3959 e6.

MAYADAS, T. N., CULLERE, X. & LOWELL, C. A. 2014. The Multifaceted Functions of Neutrophils. *Annual Review of Pathology: Mechanisms of Disease, Vol 9,* 9**,** 181-218.

MEDZHITOV, R. 2010. Inflammation 2010: new adventures of an old flame. *Cell,* 140**,** 771-6.

METZEMAEKERS, M., GOUWY, M. & PROOST, P. 2020. Neutrophil chemoattractant receptors in health and disease: double-edged swords. *Cell Mol Immunol,* 17**,** 433-450.

MILLS, C. D., KINCAID, K., ALT, J. M., HEILMAN, M. J. & HILL, A. M. 2000. M-1/M-2 macrophages and the Th1/Th2 paradigm. *Journal of Immunology,* 164**,** 6166-6173.

MISHALIAN, I., BAYUH, R., LEVY, L., ZOLOTAROV, L., MICHAELI, J. & FRIDLENDER, Z. G. 2013. Tumor-associated neutrophils (TAN) develop pro-tumorigenic properties during tumor progression. *Cancer Immunol Immunother,* 62**,** 1745-56.

MONACO, G., CHEN, H., POIDINGER, M., CHEN, J. M., DE MAGALHAES, J. P. & LARBI, A. 2016. flowAI: automatic and interactive anomaly discerning tools for flow cytometry data. *Bioinformatics,* 32**,** 2473-2480.

NAGARAJ, S. & GABRILOVICH, D. I. 2010. Myeloid-derived suppressor cells in human cancer. *Cancer J,* 16**,** 348-53.

NAJMEH, S., COOLS-LARTIGUE, J., RAYES, R. F., GOWING, S., VOURTZOUMIS, P., BOURDEAU, F., GIANNIAS, B., BERUBE, J., ROUSSEAU, S., FERRI, L. E. & SPICER, J. D. 2017. Neutrophil extracellular traps sequester circulating tumor cells via 1-integrin mediated interactions. *International Journal of Cancer,* 140**,** 2321-2330.

NEMETH, T. & MOCSAI, A. 2016. Feedback Amplification of Neutrophil Function. *Trends Immunol,* 37**,** 412-424.

NanoString, "nCounter Analysis Systems Overview" [online], https://www.nanostring.com/products/ncounter-analysis-system/ncounter-systems-overview/ (accessed 15 May 2021).

NEWBURGER, P. E., SUBRAHMANYAM, Y. V. & WEISSMAN, S. M. 2000. Global analysis of neutrophil gene expression. *Curr Opin Hematol,* 7**,** 16-20.

NYWENING, T. M., BELT, B. A., CULLINAN, D. R., PANNI, R. Z., HAN, B. J., SANFORD, D. E., JACOBS, R. C., YE, J., PATEL, A. A., GILLANDERS, W. E., FIELDS, R. C., DENARDO, D. G., HAWKINS, W. G., GOEDEGEBUURE, P. & LINEHAN, D. C. 2018. Targeting both tumour-associated CXCR2(+) neutrophils and CCR2(+) macrophages disrupts myeloid recruitment and improves chemotherapeutic responses in pancreatic ductal adenocarcinoma. *Gut,* 67**,** 1112-1123.

OHMS, M., MOLLER, S. & LASKAY, T. 2020. An Attempt to Polarize Human Neutrophils Toward N1 and N2 Phenotypes in vitro. *Front Immunol,* 11**,** 532.

QUEEN, M. M., RYAN, R. E., HOLZER, R. G., KELLER-PECK, C. R. & JORCYK, C. L. 2005. Breast cancer cells stimulate neutrophils to produce oncostatin M: potential implications for tumor progression. *Cancer Res,* 65**,** 8896-904.

RAO, H. L., CHEN, J. W., LI, M., XIAO, Y. B., FU, J., ZENG, Y. X., CAI, M. Y. & XIE, D. 2012. Increased Intratumoral Neutrophil in Colorectal Carcinomas Correlates Closely with Malignant Phenotype and Predicts Patients' Adverse Prognosis. *Plos One,* 7.

R&D Systems, "What is an ELISA" [online], https://www.rndsystems.com/resources/what-is-an-elisa-and-elisa-types#:~:text=The%20four%20main%20types%20of,indirect%2C%20sandwich%2C%20and%20competitive (accessed 15 March 2021).

RIDNOUR, L. A., CHENG, R. Y., SWITZER, C. H., HEINECKE, J. L., AMBS, S., GLYNN, S., YOUNG, H. A., TRINCHIERI, G. & WINK, D. A. 2013. Molecular pathways: toll-like receptors in the tumor microenvironment--poor prognosis or new therapeutic opportunity. *Clin Cancer Res,* 19**,** 1340-6.

ROMERO-GARCIA, S., MORENO-ALTAMIRANO, M. M., PRADO-GARCIA, H. & SANCHEZ-GARCIA, F. J. 2016. Lactate Contribution to the Tumor Microenvironment: Mechanisms, Effects on Immune Cells and Therapeutic Relevance. *Front Immunol,* 7**,** 52.

ROSALES, C. 2018. Neutrophil: A Cell with Many Roles in Inflammation or Several Cell Types? *Front Physiol,* 9**,** 113.

ROSSI, J. F., LU, Z. Y., MASSART, C. & LEVON, K. 2021. Dynamic Immune/Inflammation Precision Medicine: The Good and the Bad Inflammation in Infection and Cancer. *Front Immunol,* 12**,** 595722.

SCHINDLER, L., SMYTH, L. C. D., BERNHAGEN, J., HAMPTON, M. B. & DICKERHOF, N. 2021. Macrophage migration inhibitory factor (MIF) enhances hypochlorous acid production in phagocytic neutrophils. *Redox Biol,* 41**,** 101946.

SCHMIDT, H., BASTHOLT, L., GEERTSEN, P., CHRISTENSEN, I. J., LARSEN, S., GEHL, J. & VON DER MAASE, H. 2005. Elevated neutrophil and monocyte counts in peripheral blood are associated with poor survival in patients with metastatic melanoma: a prognostic model. *Br J Cancer,* 93**,** 273-8.

SEMERAD, C. L., LIU, F., GREGORY, A. D., STUMPF, K. & LINK, D. C. 2002. G-CSF is an essential regulator of neutrophil trafficking from the bone marrow to the blood. *Immunity,* 17**,** 413-23.

SENGELOV, H., KJELDSEN, L., DIAMOND, M. S., SPRINGER, T. A. & BORREGAARD, N. 1993. Subcellular localization and dynamics of Mac-1 (alpha m beta 2) in human neutrophils. *J Clin Invest,* 92**,** 1467-76.

SHEN, M., HU, P., DONSKOV, F., WANG, G., LIU, Q. & DU, J. 2014. Tumor-associated neutrophils as a new prognostic factor in cancer: a systematic review and meta-analysis. *PLoS One,* 9**,** e98259.

SINGHAL, S., BHOJNAGARWALA, P. S., O'BRIEN, S., MOON, E. K., GARFALL, A. L., RAO, A. S., QUATROMONI, J. G., STEPHEN, T. L., LITZKY, L., DESHPANDE, C., FELDMAN, M. D., HANCOCK, W. W., CONEJO-GARCIA, J. R., ALBELDA, S. M. & ERUSLANOV, E. B. 2016. Origin and Role of a Subset of Tumor-Associated Neutrophils with Antigen-Presenting Cell Features in Early-Stage Human Lung Cancer. *Cancer Cell,* 30**,** 120-135.

SR, W., COOK, E. J., GOULDER, F., JUSTIN, T. A. & KEELING, N. J. 2005. Neutrophil-lymphocyte ratio as a prognostic factor in colorectal cancer. *Journal of Surgical Oncology,* 91**,** 181-184.

STIDHAM, R. W. & HIGGINS, P. D. R. 2018. Colorectal Cancer in Inflammatory Bowel Disease. *Clin Colon Rectal Surg,* 31**,** 168-178.

TARDIF, M. R., CHAPETON-MONTES, J. A., POSVANDZIC, A., PAGE, N., GILBERT, C. & TESSIER, P. A. 2015. Secretion of S100A8, S100A9, and S100A12 by Neutrophils Involves Reactive Oxygen Species and Potassium Efflux. *J Immunol Res,* 2015**,** 296149.

TARIQUE, A. A., LOGAN, J., THOMAS, E., HOLT, P. G., SLY, P. D. & FANTINO, E. 2015. Phenotypic, Functional, and Plasticity Features of Classical and Alternatively Activated Human Macrophages. *American Journal of Respiratory Cell and Molecular Biology,* 53**,** 676-688.

TAVAKKOLI, M., WILKINS, C. R., MONES, J. V. & MAURO, M. J. 2019. A Novel Paradigm Between Leukocytosis, G-CSF Secretion, Neutrophil-to-Lymphocyte Ratio, Myeloid-Derived Suppressor Cells, and Prognosis in Non-small Cell Lung Cancer. *Front Oncol,* 9**,** 295.

ThermoFisher Scientific, "Controls for RNAi experiments" [online], https://www.thermofisher.com/no/en/home/life-science/rnai/synthetic-rnai-analysis/controls-for-rnai-experiments.html (accessed 8 March 2021).

URIBE-QUEROL, E. & ROSALES, C. 2015. Neutrophils in Cancer: Two Sides of the Same Coin. *J Immunol Res,* 2015**,** 983698.

VON VIETINGHOFF, S. & LEY, K. 2008. Homeostatic regulation of blood neutrophil counts. *Journal of Immunology,* 181**,** 5183-5188.

WIGHTMAN, S. C., UPPAL, A., PITRODA, S. P., GANAI, S., BURNETTE, B., STACK, M., OSHIMA, G., KHAN, S., HUANG, X., POSNER, M. C., WEICHSELBAUM, R. R. & KHODAREV, N. N. 2015. Oncogenic CXCL10 signalling drives metastasis development and poor clinical outcome. *Br J Cancer,* 113**,** 327-35.

WOSEN, J. E., MUKHOPADHYAY, D., MACAUBAS, C. & MELLINS, E. D. 2018. Epithelial MHC Class II Expression and Its Role in Antigen Presentation in the Gastrointestinal and Respiratory Tracts. *Front Immunol,* 9**,** 2144.

WU, L. Y., SAXENA, S., AWAJI, M. & SINGH, R. K. 2019. Tumor-Associated Neutrophils in Cancer: Going Pro. *Cancers,* 11.

XU, W., ZHAO, X. W., DAHA, M. R. & VAN KOOTEN, C. 2013. Reversible differentiation of pro- and anti-inflammatory macrophages. *Molecular Immunology,* 53**,** 179-186.

YOON, J., TERADA, A. & KITA, H. 2007. CD66b regulates adhesion and activation of human eosinophils. *J Immunol,* 179**,** 8454-62.

ZHANG, R., LIU, Q., LI, T., LIAO, Q. & ZHAO, Y. 2019. Role of the complement system in the tumor microenvironment. *Cancer Cell Int,* 19**,** 300.